Applied Thermal Engineering 69 (2014) 55–77

Contents lists available at ScienceDirect

Applied Thermal Engineering

journal homepage: www.elsevier.com/locate/apthermeng

A review of the case for modern-day adoption of hydraulic air compressors

Dean L. Millar [a,b,*]

[a] Mining Innovation Rehabilitation and Applied Research Corporation, Sudbury, Ontario, Canada
[b] Bharti School of Engineering, Laurentian University, Sudbury, Ontario, Canada

HIGHLIGHTS

- An improved formulation for flow in the downcomer shaft of a HAC is outlined.
- The role of gas solubility on the yield of gas and efficiency of HACs is explained.
- Estimates of efficiency for historical HACs are revised downward by ~20%.
- Efficiency can be improved back to former levels by running HACs 'hot'.
- In run-of-river HACs, gas solubility phenomena may lead to a carbon capture process.

ARTICLE INFO

Article history:
Received 7 December 2013
Accepted 4 April 2014
Available online 26 April 2014

Keywords:
Hydraulic air compressor
Ragged Chutes
Compressed air
Two-phase flow
Gas solubility in water
Engineering economics
Mine ventilation
Mine refrigeration
Carbon capture

ABSTRACT

Despite 18 reported commercial large scale deployment cases of hydraulic air compressors (HACs), the technology has fallen into demise. This paper opens by explaining that many of the reasons for this are no longer relevant in a modern context. The operating principles of HACs are reviewed and a hydrodynamic formulation is outlined so that HAC performance can be assessed by means of simulation. Simulation results confirm that HACs practically offer a close-to-isothermal gas compression and so still offer large scale gas compression utility with lower energy consumption in comparison to modern-day compression plant, even if decoupled from their opportunistic utilization of natural hydropower resources. Failure to properly account for the pressure solubility of gases in water leads to the erroneously high estimates of around 83% for the HAC mechanical efficiency for the two largest HACs built, at Victoria, MI, USA and at Ragged Chutes, ON, Canada. While still remaining only weakly coupled to the hydrodynamic simulator, simulations based on reported performance of the historical HACs, that now account for gas solubility, result in downward revision of mechanical efficiency to around 64%. Simulation results further indicate that for HACs where water is recirculated, mechanical efficiencies may be able to be increased from the new, lower estimates by i) prior solution of a salt in the circulating water or ii) increasing the temperature of HAC operation. Both measures have the effect of reducing gas solubility and hence increasing compressed air yield. An examination of the modern day economic case for HAC technology using discounted cash flow techniques concludes that they may be able to compete economically with large scale multi-stage centrifugal compressors. Two new potential application areas for HACs are presented. Firstly a deep mine ventilation air cooling concept is explained and secondly, gas solubility, that hitherto has proved problematic for HACs, is turned to advantage in a carbon capture concept.

1. Introduction

Historically, the hydraulic air compressor (HAC) has been driven only by water, held up by a dam to create relatively low head (typically 10–20 m), such that the developed hydropower is used to cause flow in openings deeper underground. Air is entrained in the water at the inlet to the sub-surface openings and is compressed

* MIRARCO Mining Innovation, 935 Ramsey Lake Road, Sudbury, ON P3E 2C6, Canada.
E-mail addresses: dmillar@mirarco.org, dmillar@laurentian.ca.

http://dx.doi.org/10.1016/j.applthermaleng.2014.04.008
1359-4311/

near isothermally as it is carried along by the deepening water flow. At depth, and with lower water velocities arising from larger cross sectional area tunnels, air bubbles have been separated out of the water flow and have been collected in a receiver space above the flowing water. Water, free of air, then passed back up a riser shaft to rejoin the natural watercourse. In principle, a HAC can produce any pressure and flow rate of compressed air required (up to around 9 bar absolute where solubility losses become significant) given large enough shafts and enough water supply with head sufficient to overcome frictional resistance in the sub-surface tunnels.

A Hydraulic Air Compressor (HAC) is thus a large scale installation, typically formed in rock tunnels, that constitutes a method of harnessing hydropower, a renewable source of energy, towards the production of compressed air. The technology was first established in 1890 in Ontario by Charles Taylor. 18 examples of the technology have been reported to have been constructed, in 9 different countries, on three different continents, mostly for mining applications [1]. The largest of these was at Ragged Chutes, on the Montreal River, 20 km south of Cobalt in Ontario, Canada. Other than a pneumatic, and subsequently, a hydraulic power assembly to move the intake head vertically up or down in response to natural watercourse head and discharge variations, these systems have no moving parts and hence have high reliability; after commissioning, the system at Cobalt operated more-or-less continuously for 70 years, operations only being interrupted twice for maintenance to the intake head. During this time, up to 25 silver mines, presumably with rather lower production rates compared with modern day practices, were supplied with compressed air from the Ragged Chutes installation by means of a distribution system comprising up to 130 km of distribution pipe work [2].

The purpose of this paper is i) to discuss the reasons why this technology fell into demise since it was first conceived and deployed over a century ago, and to revisit these reasons to establish whether or not the hurdles still hold in a modern context, ii) to explain the operating principles of HACs, iii) to set out some of the characteristics of an upgraded HAC simulation tool that can be used to undertake technical feasibility assessment of the context, iv) to examine the influence of the solubility of gases in water on the compressed air yield and mechanical efficiency of HACs, v) to explore the economic case for HACs in a modern context and vi) to present some thoughts on modern applications of HAC technology.

The contributions to the field of HACs reported in this paper are manifold. Firstly, the work reports on the use of a hydrodynamic formulation that modestly extends those reported previously in the literature by including the velocity of the air relative to the water in the air and water mixing head as a variable to be solved for, rather than an empirically determined given. Secondly, HAC configurations are proposed that do not utilise hydropower resources, but instead operate in open or closed loop circuits, driven by a pump, motivated by the close-to-isothermal, yet practical, gas compression that consumes close-to-minimum work. Thirdly, an expression for the mechanical efficiency of a HAC is presented that reflects the nearly isothermal gas compression as well as the reduced yield of compressed gas due to solubility. Mechanical efficiency is a much more important parameter in open or closed loop HAC configurations where the input energy needs to be paid for. The resulting simulation tool makes predictions of the mol fractions of oxygen in compressed air that are in excellent agreement with measurements reported in the literature over 100 years ago, for two distinct cases. Fourthly, examination of the modern day economic case for HACs indicates that they may be able to compete with contemporary multi-stage, inter and after cooled centrifugal compressors. Finally, two innovative applications of HACs are suggested: one involving cooling of deep mine ventilation air and the second involving the capture of CO_2 from industrial scale combustion plant.

2. The demise of HACs

Despite the benefit of low cost production of compressed air, Ragged Chutes is also the last reported HAC operating installation. The demise of the technology arose for 4 main reasons:

- Electricity was a far more marketable form of energy than compressed air.
- The differential solubilities of oxygen and nitrogen in water.
- The creation of leakage paths through the rock mass.
- Increased maintenance costs of the compressed air distribution network.

The review of the reasons for the demise of the technology presented in Table 1 suggests that perhaps such challenges are no longer significant issues for modern mining practice as they are either no longer relevant or can be readily mitigated. Consequently, this work makes the provisional assumption that it is appropriate to consider HACs a technology that should be revived and to investigate whether or not this century-old technique has a role to play in modern mining practice.

3. Explanation of operation

In this section, HAC system operation is explained without, initially, considering any air being inducted into the system at all. Subsequently, the principles governing air induction and the mixing of air and water below the air and water intakes are outlined. A two-phase bubbly flow predominates in the so-called 'down-comer' shaft of the HAC, and the care in design that is required to permit this flow to transition into the separation chamber/receiver at depth without significant loss is explained.

3.1. Basic water circuit

A schematic diagram of an HAC system is presented in Fig. 1, with the significant simplification that, initially, no air shall be considered inducted into the system. Water passes from an upper section of a natural water course at station 1 into a stilling dam/forebay. At the top of this dam, a weir exists to maintain the upper water level constant so that any excess, potentially seasonal, discharge is permitted to overflow to a spillway to rejoin the watercourse further downstream (at 16).

From the stilling dam, water enters the down-comer shaft at its inlet between stations 4 and 5, shown in Fig. 1 as 'bell mouthed' to minimise entrance loss (loss factor, $K = 0.02$). Between 5 and 8, water passes down the shaft overcoming the frictional resistance associated with the flow for this duct. At the same time, potential energy is reduced and converted to elevated water pressure and mass conservation and a constant shaft cross sectional area together dictate that the velocity, and thus the kinetic energy, remains constant. Having suffered an exit loss between stations 8 and 9/10, the flow enters a chamber of large cross sectional area such that the velocity of the water is slowed and any frictional loss between sections 10 and 12 is insignificant. (With air present in the system, this low velocity permits buoyant bubbles of air to rise up, across the water flow, according to Stoke's Law, and accumulate in a receiver air space, above the water, that has the same pressure as the water.)

The water flow, having suffered another entrance loss between 12 and 13, rises up the shaft while the water pressure reduces and potential energy is recovered and while frictional resistance in this riser shaft is overcome. After suffering further exit losses between 14 and 15, the water enters the downstream stilling pond/tailrace and subsequently, rejoins the natural water course at the elevation

Table 1
Reasons for the demise of HAC systems and their review in the context of modern mining practice.

Reason	Modern context of this problem
In the early 1900s, harnessing hydropower to produce electricity realised a far more flexible, and thus more marketable, form of energy.	While electricity continues to be the most attractive form of delivery of renewable energy, compressed air is still extensively used in modern mining practice. In recent years technology has evolved toward the use of (diesel-)electro-hydraulic power for rock drilling and away from compressed air. However, other uses, including actuation of ore chutes, doors etc. still means that there is significant demand. For a modern underground mining operation, such as Nickel Rim South Mine in Sudbury, Ont., Canada, electricity used in compressing air can be up to 3% of the total electricity consumed annually, estimated at 4 GWh for this mine [3].
Due to the higher solubility of oxygen than nitrogen in water, air supplied to workings had lower oxygen content in comparison to compressed air produced by mechanical means – such as reciprocating compressors. Miners complained that using compressed air from a HAC starved them of oxygen. This was at a time when mine ventilation systems still partially relied on the sub-surface compressed air distribution system to deliver fresh air to working faces.	Miners, who were still using candles and carbide lamps to illuminate workings, could tell the air was being hydraulically rather than mechanically compressed because their lamps burned less brightly. In modern times, the contribution of compressed air to ventilation budgets in sub-surface working areas is negligible. This is largely a result of regulatory innovation over recent decades driven by a technology switch away from tracked haulage systems to diesel driven trackless mining. Use of compressed air for ventilation is discouraged and really is restricted to emergency scenarios. For higher head applications considered later in this paper, higher concentrations of dissolved atmospheric gases in the riser shaft are inevitable and, overall may represent a loss of compressed air delivery. However, depressurisation, and reduced solubility, in the riser shaft will result in formerly dissolved gases coming out of solution and providing a motive effect due to bubble buoyancy.
In the case of Ragged Chutes, late in its operating life, bubbles could be discerned in the water course mid sections between intake and outlet shafts which indicated that over time, air compressed by the system had found, or had developed, leakage paths through the rock fracture network.	There are few, if any complete records of the design process for Ragged Chutes. However around 1900, when the system was designed, it seems unlikely that the air receiver chamber was specifically designed as a pressure tunnel. Consequently, modern rock stabilization practices involving both reinforcement (e.g. systematic pattern rock bolting) and rock support (e.g. shotcrete) would do much to mitigate the development of air leakage routes through the rock mass to the surface from sub-surface openings. Modern grouts, grouting practice as well as the use of spray on polymer-linings, could act to further reduce leakage potential. Despite these observations, it should also be remembered that the Ragged Chutes system operated for over 70 years, and thus, perhaps some leakage of compressed air through the discrete fracture network was inevitable.
While the actual cost of production of compressed air by HAC remained low, the costs of distributing the compressed air increased significantly over time due to progressively higher maintenance requirements as the distribution system aged.	Leakage in compressed air distribution systems remains a significant challenge for the modern mining industry. A recent study [4] undertaken for the Ontario Mining Association showed that significant cost savings can be realised by detecting and repairing leaks in compressed air systems. For Ragged Chutes, operability and serviceability of the actual air compressor was not a factor in the technology's demise. Use of an HAC does not solve the problem of leakage in an underground compressed air distribution system, however the cost associated with such leaks may be substantially lower.

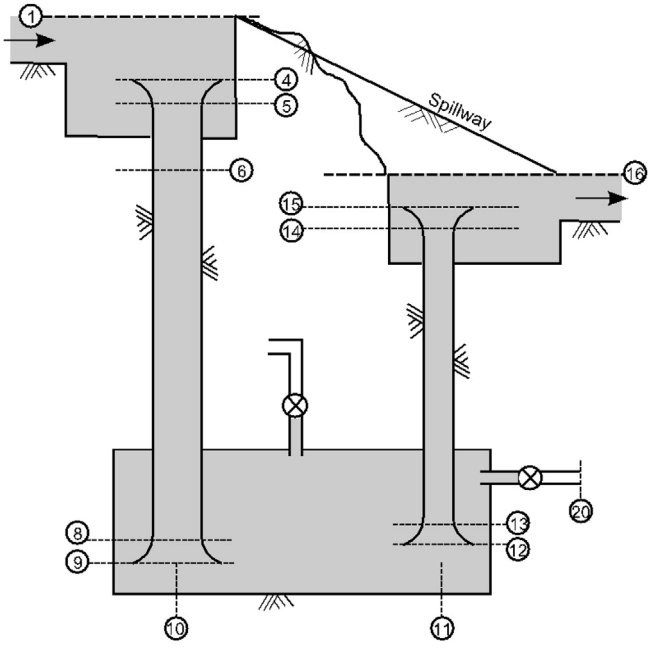

Fig. 1. Schematic of HAC arrangements, shown in a starting condition without air, compressed or otherwise, present in the system. Shaft, or duct, 4 to 9 is known as the downcomer. Shaft 12 to 15 is known as the riser.

of station 16, lower than that of station 1, but with the same (atmospheric) pressure as at station 1. Atmospheric pressures at stations 1 and 16 constitute boundary conditions of the system.

In an unregulated condition, the head available between stations 1 and 16 will result in water flowing through the subsurface openings at precisely the discharge rate that will cause all the available head to be consumed in overcoming all the various losses. The spreadsheet model presented in Fig. 2, which illustrates this condition for HAC geometry (shaft areas, lengths, depths and elevations) informed by those at Ragged Chutes, shows this discharge to be 105.665 m^3/s. With 10 m head, the total hydropower resource available is 10.3 MW and all of this power is consumed in overcoming the losses in the sub-surface. Note that the water pressure at station 9/10 is found to be 10.5 bar (152 psi).

If the discharge through the sub-surface workings is regulated to be 60 m^3/s (Fig. 3), with any excess water flowing down the spillway, the hydropower resource available to the system is 5.9 MW. 1.9 MW of this is consumed in overcoming the sub-surface losses in the flow, lower than before because the water velocities through the system are lower with the reduced discharge. 4.0 MW are available to do useful work.

In the absence of air in the system, this useful work would be dissipated through high velocity, turbulent mixing between stations 15 and 16, or, could be used to drive a hydro turbine installed somewhere in the sub-surface. If air had been admitted into the system at the intake, the work would be consumed in compressing the air to approximately 10.5 bar at station 9/10.

Atmospheric pressure	101000	Pa (abs)	Elevation of stn 9	*-110* mAD
Acceleration due to gravity	9.8091	m/s^2	Elevation of stn 15	*-10* mAD
Water density	1000	kg/m^3		
Discharge rate	105.6653	m^3/s	Total pressure loss	98091 Pa
			Total head loss	10.00 m
			Total head avail.	10.00 m
			Hydropower available	10365 kW
			Power for compression	0 kW

Stn		1	5	7	9	10	12	13	14	15
Duct width	m	*40*			*4*	*4*				*40*
Duct height	m	*4*			*6*	*6*				*4*
Diameter	m		*3*	*3*			*3*	*3*	*6*	
Area	m^2	160.00	7.07	7.07	24.00	24.00	7.07	7.07	28.27	160.00
Hydraulic diameter	m	7.27	3.00	3.00	4.80	4.80	3.00	3.00	6.00	7.27
Velocity	m/s	0.66	14.95	14.95	4.40	4.40	14.95	14.95	3.74	0.66
Elevation	mAD	**0**	-5	-108	-110	-110	-106	-14	-12	-10
KE	J/kg	0.22	111.73	111.73	9.69	9.69	111.73	111.73	6.98	0.22
PE	J/kg	0.00	-49.05	-1059.38	-1079.00	-1079.00	-1039.76	-137.33	-117.71	-98.09
Frictional loss										
Length	(m)			103		*500*		92		
viscosity	(Pa s)			0.001138		0.001137		0.001137		
roughness	(m)			*4.5E-05*		*0.01*		*4.5E-05*		
Reynolds number, Re				39412761		18585027		39437112		
Friction factor, f				0.009		0.025		0.009		
Loss	(J/kg)			33.82		25.12		30.21		
Inlet loss										
K			*0.02*				*0.02*			
Loss	(J/kg)		2.23				2.23			
Exit loss										
K					*0.02*				*0.02*	
Loss	(J/kg)				2.23				2.23	
Mixing loss										
Loss										-1.8E-07
Total loss in leg	(J/kg)	0.00	2.23	33.82	2.23	25.12	2.23	30.21	2.23	0.00
Total head loss in leg	(m)	0.00	0.23	3.45	0.23	2.56	0.23	3.08	0.23	0.00
pE	J/kg	0.00	-64.70	911.81	1031.24	1006.11	862.61	-70.04	12.85	0.00
Pressure	Pa (gauge)	**0.00**	-635	911814	1031236	1006115	862606	-70041	12853	**0.00**
	bar (gauge)	0.00	-0.01	9.12	10.31	10.06	8.63	-0.70	0.13	0.00
Sum	J/kg	0.22	-2.02	-35.84	-38.07	-63.19	-65.43	-95.64	-97.87	

Fig. 2. Spreadsheet calculations demonstrating the unregulated flow condition of a HAC system operating with 10 m head, and 110 m depth to the receiver chamber. Emboldened figures are boundary conditions; italicized figures are design variables that may be changed for different installations; the underlined figure is the water discharge solved for using a Newton Raphson iterative technique, subject to the other design and boundary conditions present within the model.

For design of a steady operating condition, HAC systems admit substantially less water than the peak natural watercourse discharge, and discharge lower than the seasonal minimum, by an amount typically dictated by abstraction regulations. For a given head and system design geometry, the system discharge can be optimally regulated such that the work available (for air compression) is maximised. Using the design geometry set out in Figs. 2 and 3, Table 2 summarises an exploration of the power available for compression as a function of the controlled discharge. Maximum hydropower available for air compression occurs at discharge rate of between 50 and 60 m^3/s.

3.2. Water and air intake head

The Ragged Chutes HAC had a downcomer shaft with twin heads (Figs. 4 and 5). Each head assembly was able to have its elevation adjusted, with continuity of the water circuit being maintained by a sleeve that passed down into the downcomer shaft. It seems that intake head design was rather poorly understood by the pioneers of HAC technology. Schulze [1] reports on two of Taylor's HACs where the intake head suffered damage shortly after commissioning during 'blow-back'. At Ragged Chutes, rather than any sophisticated independent air and water intake geometries, the elevation of the top of the intake pipes was adjusted to be 0.4 m below the water level of the intake chamber [5]. This caused sufficient churning and other turbulence of the water so that air became mixed with this water and was drawn into the system. For modern designs, HAC intake heads could follow the principles used for vacuum eductors or venturi injectors, as used in gas–liquid chemical mixing, or as in a modern day jet pump. In Taylor's design, the water would be the motive, or primary fluid that surrounds the air, or secondary fluid.

Keenan and Neumann in 1942 [6] seem to be credited with the first mathematical description of injectors/eductors, but various later sources [7–15] still present empirical or numerical explorations of the interactions between primary and secondary fluids in such devices. This makes Taylor's evident grasp of these principles of operation for design of such devices [16,17] a century ago, even more impressive.

Analysis of the hydrodynamics of the water–air intake system requires simultaneous consideration of conservation of mass, energy and momentum equations, if the losses through the intake are to be determined. Simplified approaches allowing algebraic expressions for the pressure and velocity of water and air at the exit of the intake head assembly of HACs, utilizing mass and energy conservation equations only, are presented by Rice [18], Bidini and co-

Atmospheric pressure	101000	Pa (abs)	Elevation of stn 9	*-110*	mAD
Acceleration due to gravity	9.8091	m/s^2	Elevation of stn 15	*-10*	mAD
Water density	1000	kg/m^3			
Discharge rate	60	m^3/s	Total pressure loss	98091	Pa
			Total head loss	10.00	m
			Total head avail.	10.00	m
			Hydropower available	5885	kW
			Power for compression	3967	kW

1919

Stn		1	5	7	9	10	12	13	14	15
Duct width	m	*40*			*4*	*4*				*40*
Duct height	m	*4*			*6*	*6*				*4*
Diameter	m		*3*	*3*			*3*	*3*	*6*	
Area	m^2	160.00	7.07	7.07	24.00	24.00	7.07	7.07	28.27	160.00
Hydraulic diameter	m	7.27	3.00	3.00	4.80	4.80	3.00	3.00	6.00	7.27
Velocity	m/s	0.38	8.49	8.49	2.50	2.50	8.49	8.49	2.12	0.38
Elevation	mAD	**0**	-5	-108	-110	-110	-106	-14	-12	-10
KE	J/kg	0.07	36.03	36.03	3.13	3.13	36.03	36.03	2.25	0.07
PE	J/kg	0.00	-49.05	-1059.38	-1079.00	-1079.00	-1039.76	-137.33	-117.71	-98.09
Frictional loss										
Length	(m)			103		*500*		92		
viscosity	(Pa s)			0.001138		0.001137		0.001137		
roughness	(m)			*4.5E-05*		*0.01*		*4.5E-05*		
Reynolds number, Re				22379781		10553151		22393608		
Friction factor, f				0.009		0.025		0.009		
Loss	(J/kg)			11.09		8.10		9.90		
Inlet loss										
K			*0.02*				*0.02*			
Loss	(J/kg)		0.72				0.72			
Exit loss										
K					*0.02*				*0.02*	
Loss	(J/kg)				0.72				0.72	
Mixing loss										
Loss										66.11468
Total loss in leg	(J/kg)	0.00	0.72	11.09	0.72	8.10	0.72	9.90	0.72	66.11
Total head loss in leg	(m)	0.00	0.07	1.13	0.07	0.83	0.07	1.01	0.07	6.74
pE	J/kg	0.00	12.37	1011.62	1063.42	1055.31	982.46	70.12	83.55	0.00
Pressure	Pa (gauge)	**0.00**	121	1011619	1063417	1055315	982458	70117	83552	**0.00**
	bar (gauge)	0.00	0.00	10.12	10.63	10.55	9.82	0.70	0.84	0.00
Sum	J/kg	0.07	-0.65	-11.74	-12.46	-20.56	-21.28	-31.19	-31.91	

Fig. 3. Spreadsheet calculations demonstrating the condition of a HAC system operating with 10 m head, and 110 m depth to the receiver chamber and discharge regulated to 60 m^3/s.

workers [19,20] and Aissa [21]. The approach adopted in this work is to use all three (one-dimensional) conservation equations, applied to water and air streamlines, so that water and air pressure, velocity and temperature can be determined at the point where the two fluids meet (Station 6 in Fig. 6).

Determinations of the frictional losses, for convergent motive fluid ducts with multiple air intake pipes, of uniform section interrupting this flow, are undertaken in this work (a single intake tube is shown in Fig. 6, for simplicity). The equations are solved simultaneously, using a Newton–Raphson technique, with numerical determination of derivatives for formulation of the Jacobian in the solution procedure. For the water space between station 5 and 6 (Fig. 6), the water and air intake assembly is discretised into short sections so that the intake conditions for each segment, taken together with the duct segment geometry, determine the segment outlet conditions and the losses incurred in the segment. This discretisation approach is undertaken for convergent or divergent ducts only, because: under the conditions of non-uniform cross sections, non-axial duct wall pressure forces and non-axial forces arising from wall friction arise in the momentum conservation equations applied to a fluid control volume involving the duct walls.

3.3. Air and water mixing zone

Detailed analytical understanding of the air and water mixing process in venturi inductor devices appears to remain elusive, a conclusion supported by Field and Hrnjak [22] in their detailed review of empirical relations governing mixing of two fluid streams in such devices. However, sufficient understanding exists on the basis of a rather large body of historical experimental evidence, and newer empirical results derived from computational fluid dynamics studies, such that these devices can be reliably designed or selected. The seminal work on this topic was conducted by Keenan and Neumann [6] in 1942. Their work relies on assumptions of either constant pressure, or constant cross sectional area across the mixing zone. In this and other precedent works on HACs simulation [18–21], the detailed mechanisms of gas bubble formation and migration within a primary, motive, fluid between stations 6 and 7 in Fig. 6 are sidestepped by mass, energy and momentum conservation formulations applied across a mixing zone that is conceptually 'thin'. Effectively, air bubbles are instantaneously assimilated and distributed within the motive fluid.

In this work, following the procedure of Christi and Moo-Young [23], a uniform air bubble diameter is assumed, and estimated

Table 2
HAC system performance for system of Figs. 2 and 3.

Discharge (m^3/s)	20	30	40	50	60	80	100	105.6
Total hydropower available (MW)	1.962	2.943	3.924	4.905	5.885	7.847	9.809	10.365
Hydropower used to overcome losses (MW)	0.074	0.245	0.575	1.116	1.918	4.519	8.793	10.365
Hydropower available for compression (MW)	1.888	2.698	3.349	3.789	3.967	3.328	1.016	0

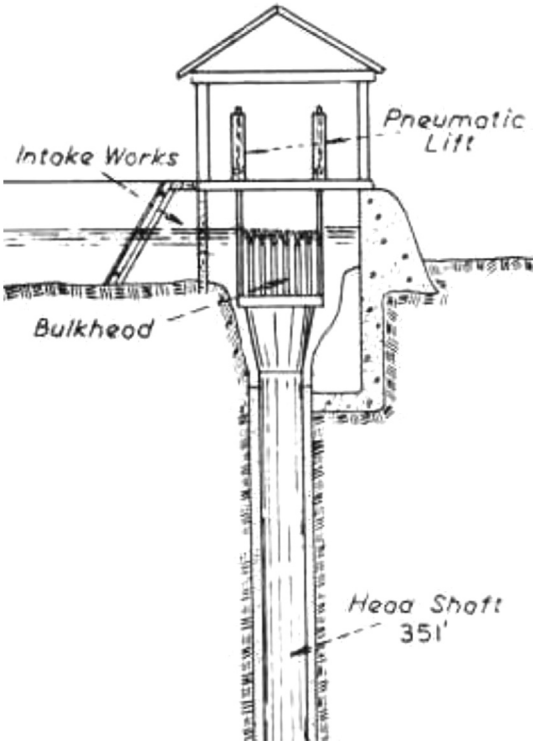

Fig. 4. Air and water intake arrangement at the Ragged Chutes HAC. Source: Schulze [1]. Two such heads were installed, each with 72, 0.36 m diameter intake pipes [29].

using empirical relations established by Akita & Yoshina [24] for homogeneous two phase flow, or Wilkinson [25] for heterogeneous two phase flow. The flow regime is determinable with knowledge of the water and mass flow rates, and the mixing device geometry (see Ref. [22] for details). After determination of the air bubble diameter, the bubble volume, mass and flux (number of bubbles per second) can then be estimated. In addition, knowledge of the bubble diameter permits estimation of the initial velocity of the gas bubbles relative to the air, at the exit of the mixing zone and hence also at the entrance to the main downcomer shaft section. In prior work, this value, which reflects the phenomena of drag on the gas bubble from the primary, motive fluid, as well as the buoyancy of the bubble within it, is assumed to be 0.244 m/s; this is a value that has its roots in experimental investigations undertaken by Rice [18]. In this work, rather than simply adopt this value similarly, the value of 0.244 m/s is used as the initial estimate in an iterative numerical technique that solves for the initial velocity of gas (air) bubbles relative to water for each set of head and discharge conditions explored. If the velocity of the water falls below this value, the air bubbles will not be drawn down into the shaft because the drag force is insufficient to overcome the buoyancy force.

Fig. 5. Showing, now derelict, twin intake heads for the HAC at Ragged Chutes.

3.4. Two phase bubbly flow in the downcomer shaft

Analysis of the flow in the down-comer shaft between stations 7 and 8, in Fig. 6, requires the flow to be considered two phase. The ratio of mass flow rates of air and water found from the earlier stages of analysis, almost invariably results in a so-called heterogeneous bubbly two-phase flow and a mass flow rate ratio between 500:1 to 2000:1 arises across the system 1-2-6, in Fig. 6. Volumetric flow rate ratios close to the intake are around unity.

The air bubbles entrained in, and drawn along with, the motive fluid (water) are compressed by this fluid as it becomes pressurised with depth. As the bubbles become compressed, the volume available to be occupied by the incompressible liquid phase increases, and consequently, its velocity reduces as it progresses down the shaft between stations 7 and 8.

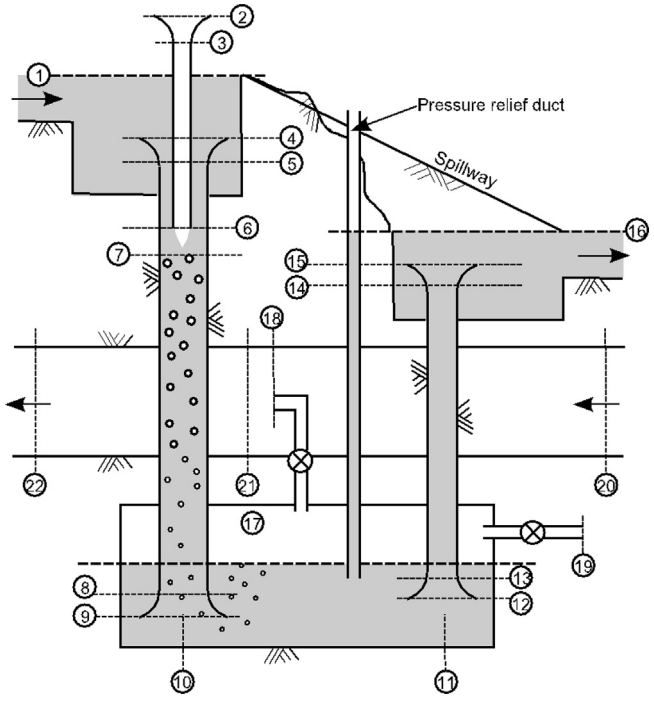

Fig. 6. Schematic diagram of an HAC in operation.

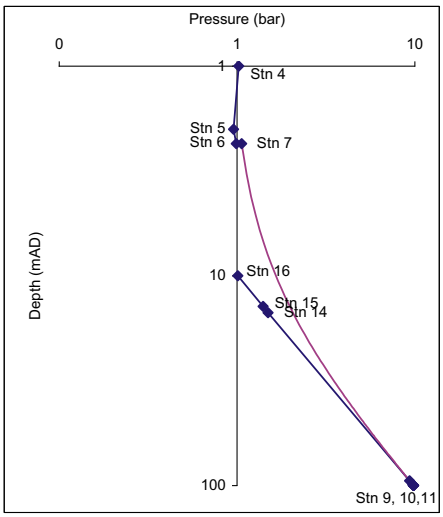

Available head	10	m
Air tube diameter	0.3	m
Number of air tubes	80	
Water discharge	10	m^3/s
Gas regulator at 6	8%	
HAC free air delivery	4.5	m^3/s

Stn	P abs (bar)	T (K)	v (m/s)	Depth (m)
1	1.010	283.14	4.0	0.000
4	1.022	283.14	3.2	1.000
5	0.958	283.14	3.0	2.000
6	0.992	283.14	3.0	2.345
7	1.065	283.14	3.0	2.345
8	9.363	283.16	3.0	95.000
9	9.836	283.16	3.0	100.000
10	9.845	283.16	4.4	100.000
11	9.843	283.16	4.4	100.000
12	9.838	283.16	3.4	100.000
13	9.738	283.16	3.2	99.000
14	1.496	283.16	3.2	15.000
15	1.403	283.16	4.0	14.000
16	1.012	283.16	4.0	10.000

Fig. 7. HAC System X. Pressure versus depth below intake level for a HAC with 100 m deep, 3 m diameter downcomer and riser shafts, 10 m head and 10 m^3/s discharge. The system delivers 3.8 kg/s air (free air delivery of ~10,000 cfm) at 9.8 bar absolute (128 psig).

Typical bubble sizes computed are in the range 1–5 mm at station 7. As the two phases are intimately mixed, the heat capacity of water is around four times that of air, and the mass flow of water is $\sim 10^3$ times that of the air, heat transfers from air to water are taken to occur sufficiently rapidly that the air compression process can be considered isothermal. This is a significant advantage of a HAC relative to other types of mechanical compressor. Isothermal compression is the minimum work compression of any gas, and is why mechanical compressor assemblies are frequently multistage, and are equipped with intercooling and aftercooling heat exchangers. For some air compressor installations, compressed air is aftercooled using so-called *direct contact* aftercoolers that are columns in which the compressed air is mixed with cooling water, with air–water separation and air drying stages following. In air liquefaction plants, direct contact aftercoolers are also used to remove carbonaceous materials and other airborne contaminants that may oxidize violently when exposed to high concentrations of oxygen.

With isothermal compression of the gas (air) phase, although the losses are minimised they still exist, and are incurred at the expense of the hydropower driving the system. In this formulation, two types of loss are considered in down-comer segmental lengths. Losses due to drag on bubbles are quantified, as are losses arising from the frictional resistance of the two phase flow on the shaft walls. As the shaft walls also comprise part of the control volume envelope for down-comer shaft segments, these terms appear in the momentum conservation equation. Both terms affect the internal energy of the two-phase energy conservation equation. The velocity is solved for each phase separately, whereas the pressure and temperature estimates for each phase are taken to be the same.

3.5. Remaining branches of the HAC circuit

Once the flow reaches the stilling chamber/receiver at stations 9/10, the velocity of the flow is reduced appreciably through a

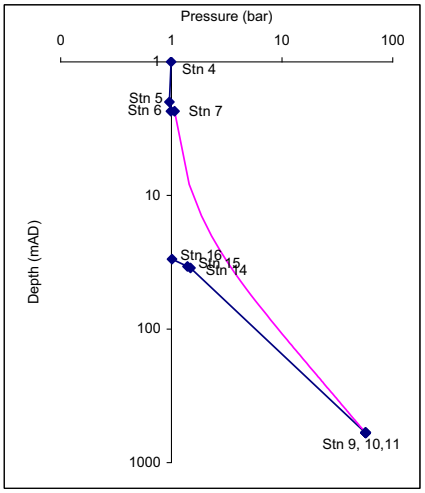

Available head	30	m
Air tube diameter	0.3	m
Number of air tubes	70	
Water discharge	15	m^3/s
Gas regulator at 6	27%	
HAC free air delivery	13.4	m^3/s

Stn	P abs (bar)	T (K)	v (m/s)	Depth (m)
1	1.010	283.14	4.0	0.000
4	0.995	283.14	3.2	1.000
5	0.960	283.14	3.0	2.000
6	0.994	283.14	3.0	2.345
7	1.071	283.14	3.0	2.345
8	56.590	283.21	3.0	595.000
9	57.075	283.21	3.0	600.000
10	57.095	283.21	4.4	600.000
11	57.090	283.21	4.4	600.000
12	57.080	283.21	3.4	600.000
13	56.977	283.21	3.2	599.000
14	1.491	283.21	3.2	35.000
15	1.403	283.21	4.0	34.000
16	1.013	283.21	4.0	30.000

Fig. 8. HAC System Y. Pressure versus depth below intake level for a HAC with 600 m deep, 3 m diameter downcomer and riser shafts, 30 m head and 15 m^3/s discharge. The system delivers 11.2 kg/s air (free air delivery of ~28,500 cfm) at 57.1 bar absolute (813 psig).

significant increase in the cross sectional area for flow implied by the chamber geometry, 10 to 11. Water passes to the riser shaft at station 12, assuming that all air bubbles have completed their buoyant migration to the water surface in the receiver plenum, station 17, where the air bubbles are assumed to coalesce with the body of compressed air. The water suffers further frictional and minor (shock) losses through the riser shaft 12 to 15. The water pressure where the upcast water rejoins the watercourse is predicted by the model and the system control variables are manipulated such that this pressure is atmospheric. Pressure, temperature and velocity variables have been computed at the station locations 1 to 16 (Fig. 6) and found to be identical to those of Bidini [19] for the same simulation cases when their simplified air intake, water–air mixing and friction and drag models for the two-phase flow in the shaft are adopted. Pressure versus depth plots, and other predicted steady state performance data for 100 m deep and 600 m deep, 3 m diameter HACs, are presented in Figs. 7 and 8 that use the more refined model of the current work.

4. Summary of precedent experiences of hydraulic air compressors

According to Langborne [5], HACs have their roots in the trompe, a device that was used by Italians for the production of iron in blast furnaces in the 16th Century. Thorkelson [26] reports that it was Joseph Frizzell to whom the first recognisable HAC, as a type of inverted siphon, can be attributed in 1877 [27]. Other pioneers of the technology were Baloche and Krahnass who invented their compressor in 1885, and Thomas Arthur who patented his HAC compressor design in 1888 [1]. Charles Taylor installed his first HAC at Magog in Quebec in 1896 [28,29]. From that time, from various sources, 18 confirmed cases of HAC installation with 3 additional unconfirmed instances can be compiled, as has been done by Langborne [5], reproduced in Table 3.

Undoubtedly the two most sizeable were those at Victoria Mine in Michigan, U.S., and at Ragged Chutes, near Cobalt, Ontario (Fig. 9). According to Table 3, they produced 16.5 m^3/s FAD @ 8.07 bar(g) and 18.9 m^3/s @ 8.27 bar(g), respectively. To put these figures in context, the largest of Ingersoll Rand standard centrifugal air compressors, the Centac 5CII, can produce 14.2 m^3/s @ 10.3 bar(g) and has a nominal rated power of 4.6 MW [34]. At the time of writing, Atlas Copco is recognised as the world's leading producer of air compressors. Their GT153 system, comprising two, 3 stage centrifugal compressors can deliver 91.7 m^3/s FAD at 5.3 bar(g) (nominal rated power estimated at 30 MW) and, in 2009, was the largest compressor Atlas Copco's Gas and Process division had ever supplied [35], with a contract value of 63.5 million SEK (approximately CAD 9.5 million in 2013 values).

5. A modern taxonomy for hydraulic compressors

The prior experiences of installation of HACs each opportunistically exploited a spatial coincidence of an available hydropower resource and demand for compressed air. The name 'Ragged Chutes' originally referred to a waterfall section of the Montreal River with a drop of elevation of around 16.5 m. The facility met demand for compressed air from silver mines in the town of Cobalt, 13 km distant. In a modern context, away from the coast, similar spatial coincidences may be rather rare. In order to render the application of HACs independent of the presence of a suitable hydropower resource, modifications in HAC design, in comparison to the earlier schemes, must be considered.

A progression of design variants are schematically illustrated in Fig. 10. Taylor's HAC concept is illustrated on the LHS of Fig. 10, and is referred to as a '*run-of-river or tidal*' HAC. A HAC can be designed to utilise the relatively low tidal head developed behind a barrage located in a macrotidal regime. Intake gases that dissolved in the water as it descended and became pressurised in the downcomer shaft would come out of solution as the water ascends in the riser shaft and the pressure reduces. This formerly dissolved gas may be collected within a canopy at the top of the riser shaft and delivered to C, while the water would rejoin the watercourse at E.

The central schematic of Fig. 10 indicates that water can be pumped from a lower reservoir, where water from the riser shaft is delivered, to an upper reservoir, or header tank, where it may pass back into the downcomer. This spatially extended arrangement, which is referred to as an "*open-loop, pumped*" HAC, has the advantage that Taylor's water/air inlet head may be adopted, and that there is an opportunity for cooling the circulating water in and between the reservoirs and at the transfer points. Gas coming out of solution in the riser shaft may again be collected in a canopy at the top of the riser shaft and delivered to C.

Table 3
Chronologically listed examples of HAC installations. Reproduced from, and sources indicated by, Langborne [5]. Air pressure is gauge.

No.	Year	Location	Available head		Water flowrate		Free air delivery		Air pressure		Eff.
			(m)	(ft)	(m^3/s)	(ft^3/min)	(m^3/s)	(ft^3/min)	(kPa)	(psi)	(%)
1	1896	Dominion Cotton Mills, Magog, Quebec, Canada [28]	6.58	21.6	2.90	6183	0.67	1419	359	52	55
2	1898	Ainsworth, British Columbia, Canada [28,1]	32.77	107.5	2.00	4200	2.41	5100	600	87	53
3	1898	Dillingen Ironworks, Dillingen, Sear, Germany [1]	1.80	5.9	0.77	1627	0.144	296	124	18	79
4	1901	Cascade Range, Washington State, USA [1]	13.72	45	1.40	3000	0.76	1620	586	85	
5	1902	Norwich, Conn., USA [28]							559	81	
6	?	Peru [29]									
7	1903	Glanzenberg Mine, Nr Siegen, Germany I [30,1]	40.00	131	0.014	30	0.019	40.5	811	117	74
8	1903	Glanzenberg Mine, Nr Siegen, Germany II [30,1]	50.00	164	0.015	31	0.0245	51.9	709	103	70
9	1903	Glanzenberg Mine, Nr Siegen, Germany III [30,1]	17.00	55.8	0.014	30	0.0082	17.4	709	103	70.2
10	1904	Trent Canal Lift Lock, Peterborough, Ontario, Canada [1]	2.74	9			0.14	300	193	28	
11	1905	Holzappel, Germany [1]	117.04	384	0.018	38	0.072	152	627	91	66
12	**1906**	**Victoria Mine, Ontonagon County, Michigan, USA [5,31]**	**21.60**	**71**	**21.20**	**45000**	**16.5**	**35000**	**807**	**117**	**82**
13	1907	Royal Mine Inspection Plant, Clausthal, Germany [30,1]	99.30	325	0.05	113	0.17	353	510	74	77
14	1908?	Zeche Victor Rauxel Mine, Dortmund, Germany [30,1]	82.00	269	0.07	141	0.17	350	607	88	73
15	1909	Royal Mine Inspection Plant, Grund, Germany [1]	36.00	118	0.16	333	0.193	408	607	88	88
16	**1909**	**Ragged Chutes, Nr Cobalt, Ontario, Canada [17,32]**	**16.50**	**54**	**22.70**	**48000**	**18.88**	**40000**	**827**	**120**	**83**
17	1915	Persberg, Sweden [1]	29.57	97	0.003	5			689	100	45-57
18	1924?	Cumberland, England [1]									
19	1925	Falun, Sweden [33]	47.85	157	0.18	381	0.6	1271	758	110	46-52
20	1929	Saragossa, Spain [1]	1.83	6	2.80	6000			103	15	
21	1929	Nigeria, Tin mine [1]									

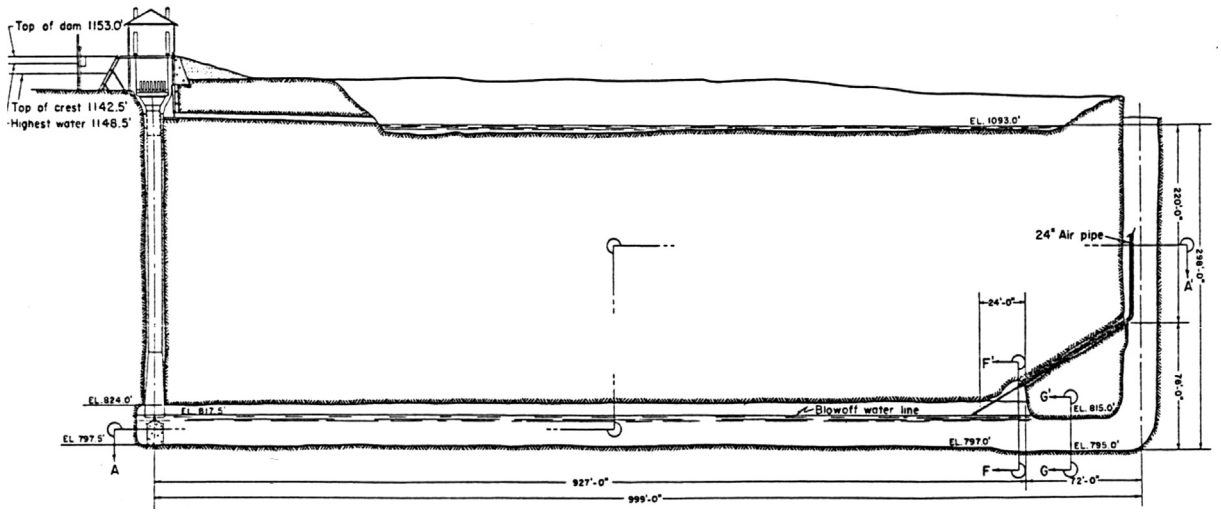

Fig. 9. Section through the HAC installation at Ragged Chutes, Cobalt, Ontario. Source: Schulze [1].

The RHS schematic of Fig. 10 is more compact, and is referred to as a '*closed-loop*' HAC. It differs from the open-loop HAC in two respects. Firstly, Taylor's air intake system must be replaced with one that can operate within a circuit that is pressurised throughout. This could be achieved with the use of a venturi injector, or eductor, (A) which is illustrated, although other arrangements are possible. Secondly, the passive separation mechanism for low pressure gas that has come out of solution in the riser shaft (C) is replaced by a cyclone gas–liquid separator. The pump used to circulate the water is of approximately the same rating as that of the open-loop pumped HAC and is assumed to develop the same head as that evident between the reservoirs of the open-loop HAC. Continued circulation of water in the closed loop system would lead to a gradual increase in the water temperature (although the residence time of the gas in the downcomer means that it would continue to approximate an isothermal compression). A feature not illustrated in the closed loop HAC, Fig. 10, RHS, is a heat exchanger that is required to remove heat from the water to maintain its temperature constant. Given that the design progression is presented as a means of overcoming a dependence on an available water source, a cooling system that ultimately dumps heat to ambient air is envisaged.

A significant advantage of Taylor's Ragged Chutes HAC layout (Figs. 9 and 10 LHS) is that the horizontal separator/receiver chamber provides a facility for compressed air energy storage (CAES). In a modern context, a decision to develop a separator/receiver chamber of similar scale and dimensions would depend on the relative economics of alternatives for compressed air storage. The capital cost of excavating this chamber, which was ~300 m long at Ragged Chutes, dominates the total capital cost of the total installation. In Ontario, as well as other jurisdictions worldwide, there are significant economic benefits associated with electricity demand reduction [36] or improved integration of

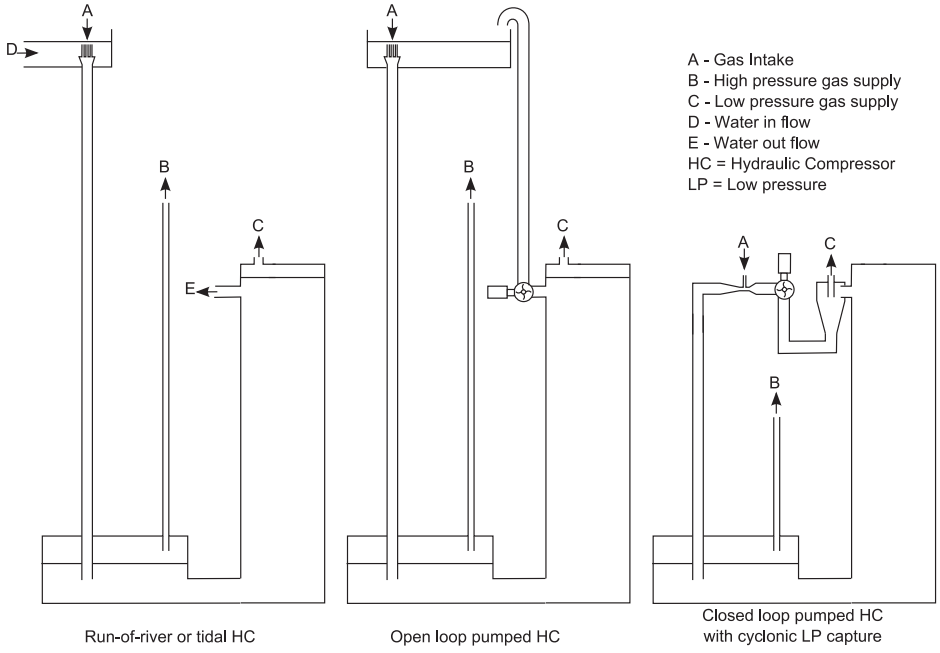

Fig. 10. Schematics illustrating a HAC design progression from Taylor's HAC to a closed loop, pumped, HAC.

renewable energy resources [37] which mean that designs incorporating large scale CAES may be preferred on economic grounds. Where there is no significant requirement for storage of compressed air in the sub-surface, the downcomer shaft may be arranged co-axially within the riser, with the compressed air separated actively by a high pressure cyclone located at depth.

A parallel set of schematics indicating further HAC design progressions each adopting co-axial downcomer and riser arrangements are shown in Fig. 11. These are presented to show how the capital costs of an HAC installation may be approximately halved, in comparison to Taylor's arrangements at Ragged Chutes. There is precedent for co-axial HAC arrangements. Taylor utilised such a system in his design for the HAC installed within the Trent Canal Lift Lock, Peterborough, Ontario, in 1904. Fig. 12 shows a photograph of a modern liquid–gas cyclone separator used in well-head oil and gas metering.

The choice of which of the HAC schematics (Figs. 10 and 11) are adopted depends upon:

1) whether there is a requirement for appreciable compressed air storage, in which case a non-coaxial arrangement may be preferred.
2) whether or not a natural hydropower resource is located close enough to the compressed air demand centre, and if so, one of the run-of-river/tidal arrangements may be preferred.
3) whether or not there is sufficient vertical relief close to a demand centre to support an open-loop system when a natural hydropower resource is not available, in which case an open-loop system may be preferred.

When there is no natural water course available or accessible and insufficient vertical relief available at the demand centre, one of the closed-loop HAC systems may be preferred.

6. The influence of gas solubility

The principal design variables for HACs are the available head, H, and the choice of depth for the separation chamber or separation cyclone below the water level of the tailrace, $z_{\text{tailrace}} - z_{\text{separator}}$. The latter determines the pressure of the service air. After these, the single most important phenomenon affecting the efficacy of the installations is the solubility of gas species in water. The reports of historical HACs (e.g. Ref. [1]) provide explanations for the reduction of oxygen concentration in the expanded compressed air, but there is little or no mention of the fact that the same phenomenon accounts for appreciable loss of compressed air from these installations. Air dissolved in the water that is separated at depth provides a mechanism for compressed air to escape the receiver plenum. The leakage has a direct bearing on the mechanical efficiency of the installation, a key factor to determine for design and economic assessment.

If equipped with observations of the atmospheric pressure, P_{atm}, the river and air temperatures T and the mass flow rates $\dot{m}$ of air (subscript G) and water (subscript W) as well as the water density ρ_W, with the principal design variables chosen or known, it is possible to establish the indicated useful work imparted to the air, and then the mechanical efficiency for the compressor can be established:

$$\eta_{\text{mech}} = y \cdot \frac{\int V \mathrm{d}P}{w_{12}} = y \cdot \frac{R(T_{\text{river}} + \delta T - T_{\text{atm}}) \frac{\ln\left[\left(\rho_W g\left(z_{\text{tailrace}} - z_{\text{separator}}\right) + P_{\text{atm}}\right)/P_{\text{atm}}\right]}{\ln((T_{\text{river}} + \delta T)/T_{\text{atm}})}}{C_{pG}(T_{\text{river}} + \delta T - T_{atm}) + \frac{\dot{m}_W}{\dot{m}_G}[C_W \delta T - gH]} \tag{1}$$

In the second factor of the RHS of the equation for η_{mech}, the numerator is the polytropic flow work and the denominator is the input work from the water to the air, both per unit mass of air (J/kg). C_{pG} and C_W are the heat capacities of the air and water respectively. The expression for the mechanical efficiency contains a term δT which is the small temperature difference (typically a rise) that occurs in the water due to the heat transferred from the air during its compression:

$$\delta T = \frac{\frac{\dot{m}_W}{\dot{m}_G} 2gH - C_{pG}(T_{\text{river}} - T_{\text{atm}})}{C_{pG} + \frac{\dot{m}_W}{\dot{m}_G} C_w} \tag{2}$$

This arises from a heat balance between the water process, which is not quite isothermal, and the air process, which is generally polytropic. If the air mass flow rate, $\dot{m}_G$ is a value that applies at the

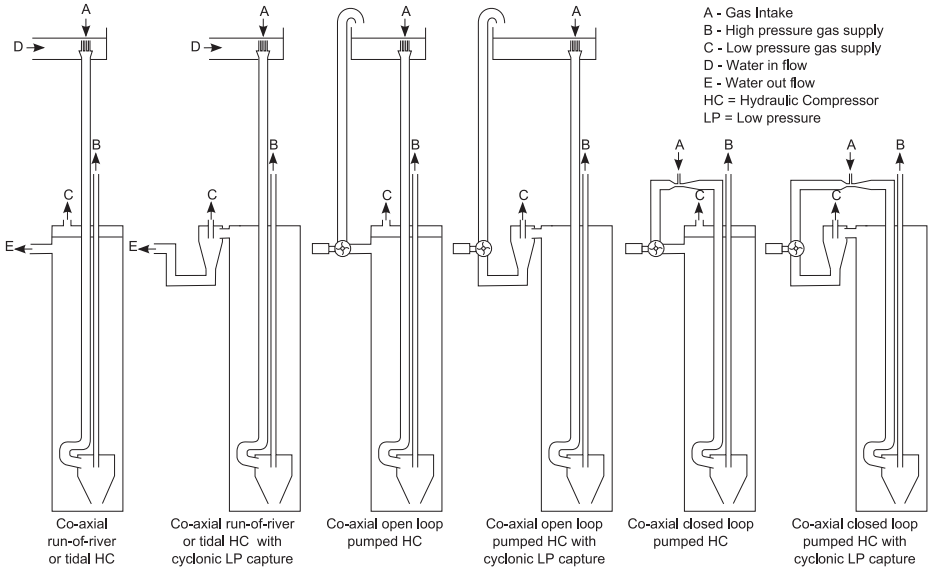

Fig. 11. A progression of design schematics for co-axial HACs, from those utilising a natural hydropower resource (LHS) to closed-loop, pumped HACs (RHS).

Fig. 12. Gas–Liquid Cylindrical Cyclone (GLCC) installed at Caltex Pacific Indonesia (CPI), Minas, Indonesia (reproduced from Wang [38]). The cyclone is 1.5 m in diameter and 6.1 m in length is designed to separate liquid crude oil and natural gas for well head metering purposes. It was nominally designed for liquid flow rates of 0.33 m^3/s and gas flow rates of 23.3 m^3/s at 11.7 bar.

Table 4
Solubility co-efficients compiled by Sander [39] for common gases.

Gas species	A_i [(mol/L)/atm]	C_i [K]
N_2	0.00061	1300
O_2	0.0013	1500
Ar	0.0014	1100
CO_2	0.035	2200

outlet of the compressor, then the factor, y, the mass yield of compressed air (% mass/mass) has a value of 100%. If $\dot{m}_G$ is metered at HAC inlet, y must be determined.

For the solubility process of gas species in water, Henry's Law (see for example, the useful compilation of Henry's Law constants in Ref. [39] or [40]), which governs the pressure solubility of gases, can be described:

$$p_i = K_i x_i \tag{3}$$

where p_i is the partial pressure of the gas species i in the gas phase, K_i is Henry's constant for species i and x_i is the maximum, equilibrium, mol fraction (concentration) of the species in the solvent (water), or the solubility. K_i can be expressed as a function of absolute temperature, T:

$$K_i = A_i \cdot \exp\left(C_i\left(\frac{1}{T} - \frac{1}{298.15}\right)\right) \tag{4}$$

where A_i and C_i are gas species specific constants, with values given in Table 4, provided by Ref. [39].

Gases dissolve in water to occupy the intermolecular space between water molecules, being held there by weak van der Waals forces (e.g. N_2, Ar), slightly stronger electronic interactions (e.g. O_2) or by much stronger hydrogen bonding which may complex the solute and hydrate it (e.g. CO_2). In the case of CO_2 a small fraction (<1%) of the dissolved gas may disassociate to form H_2CO_3, a weak acid. In general, the stronger the holding force, the greater is the solubility of the gas. In engineering units of g/kg H_2O (Fig. 13), the solubility of CO_2 is two orders of magnitude higher than that of N_2 or O_2.

Using the above gas solubility relations water at the intake of a HAC may contain the following quantities of dissolved gases: N_2 0.01554; O_z 0.01039, Ar 0.00059, CO_2 0.00079 g/kg H_2O if assumed at equilibrium with atmospheric concentrations of the same species: N_2 0.78084, O_2 0.20946, Ar 0.00934, CO_2 0.00039 mol/mol (=vol/vol). For constant pressure, Fig. 13, RHS shows that the solubility of these atmospheric gases in water reduces as the temperature increases. In a run-of-river HAC, the temperature of the water remains approximately constant (δT values are typically of order 0.1 K), and as the pressure increases, so the solubilities of all gas species in the entrapped air bubble increase (Fig. 13, LHS). With an increase in pressure, equilibrium between gas and water phase concentrations will be disturbed, and there is thus potential for mass transfers of the gas solute, enveloped (isolated from the atmosphere) by the water, to the water solvent. Assuming the gas dissolution kinetics become complete with instantaneous incremental increase in water, and hence gas, pressure, a revised equilibrium concentration of the solute in the water can be established and the corresponding necessary mass transfers from the air bubble can be computed. With a further assumption of 100% separator efficiency, an estimate of the yield, y, of compressed air can be established, when the computations are tracked to a pressure corresponding to that expected in the separation chamber. This pressure can be estimated accurately from knowledge of

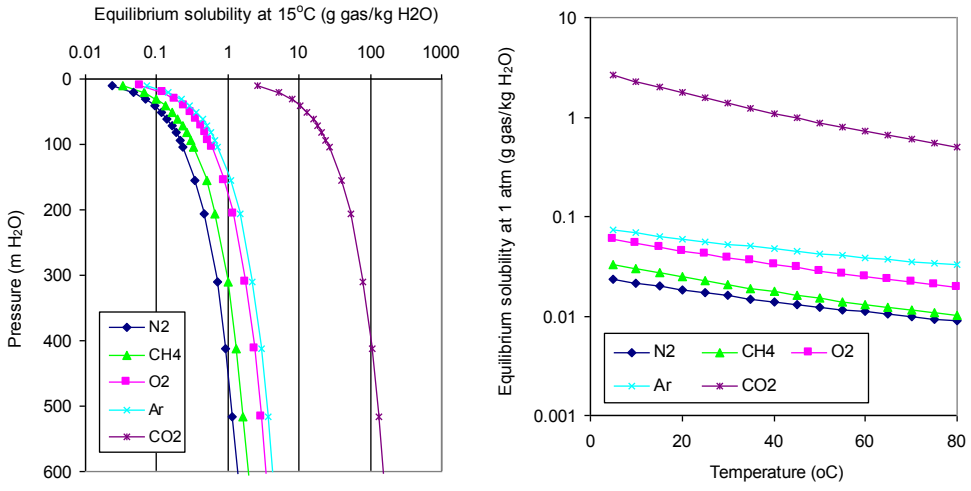

Fig. 13. Variation of common gas species in water with pressure (LHS) and temperature (RHS).

$z_{tailrace} - z_{separator}$. Chen and Rice [41] investigated gas/water solubility kinetics in their hydrodynamic model of HAC performance. However consideration of the residence time of air and water in the separation chambers of Taylor's large scale HACs strongly supports the notions that i) any transient solubility behaviour will be complete by the time that the water phase enters the riser shaft and ii) the revised equilibrium solubility condition predicted by the model described herein will be established.

Predictions from the model developed for gaseous and liquid phase solute concentrations can be compared with the value of 0.177 mol/mol of oxygen in the compressed air obtained through testing of the compressed air at the Victoria Mine HAC using a sample gathered in March 1907 by McNair and Koenig [42]:

> "*Determinations by means of a Hempel pipette, charged with thin sticks of phosphorus, showed an oxygen content of 17.7 volumes to the 100 volumes of compressor air, whereas in 100 volumes of normal air there are about 21.0 volumes of oxygen. A recently published analysis of the air from the Cobalt compressor gives 17.7 volumes of oxygen to 100 of air.*"

Schulz [1] presents the report of practical investigations of HAC performance undertaken at the Victoria Mine HAC by Sperr and Hood in May 1906. In the three performance trials, the rates of water and air entering one of the three downcomer shafts were determined, but water and air temperatures were not recorded. Consequently, the May temperature of 12 °C from the Ontonagon River near Rockland, MI [43], was adopted as the HAC water temperature and the May mean air temperature in Ontonagon, MI, adopted was 10.9 °C. Assuming the yield of compressed air as 100%, as the water flow rate increased from 18 m^3/s to 18.5 m^3/s to 21 m^3/s, the mechanical efficiency computed assumed values 73.78%, 82.37% and 82.48% respectively, offering good agreement with the hitherto accepted value for the Victoria HAC efficiency of 83% (Table 3). However, after the compressed air yield is taken into account (because the air was definitely metered at input), the corresponding mechanical efficiencies are 56.01%, 64.51% and 64.49%.

It is of historical interest that Charles Taylor had a wager with the owners of Victoria Mine that was based on the as-built performance of the HAC he supplied to them. For every 3% efficiency points lower than 70%, Taylor would lose $1000 of his fee. On the basis of the tests reported (reproduced in Ref. [1]), Taylor won the bet. This was a direct consequence of Sperr and Hood measuring the air flow at inlet and ignoring the (inevitable) solubility loss.

In March the water and air temperatures at the same location are quite different at 4 °C and −4 °C respectively [43]. With HAC water flow rate of 21 m^3/s and air ingestion rate of 20 kg/s, the mechanical efficiency of the Victoria HAC is predicted to be 58.26%, substantially lower than the value of 64.49% applying at the time of the year when Sperr and Hood conducted their performance tests. Importantly, the mol fraction of oxygen predicted to be in the compressed air for conditions corresponding to the time when McNair and Koenig took their compressed air samples is 0.176 mol/mol (Fig. 14). The mole fraction of oxygen in the compressed air is insensitive to the temperature of the intake air, but, as Table 5 shows, it is sensitive to the intake water temperature and the mass flow ratio, $\dot{m}_W/\dot{m}_G$.

For the simulation presented in Fig. 14, it is clear from Table 5, that if we wished to obtain the value of 0.177 exactly, the

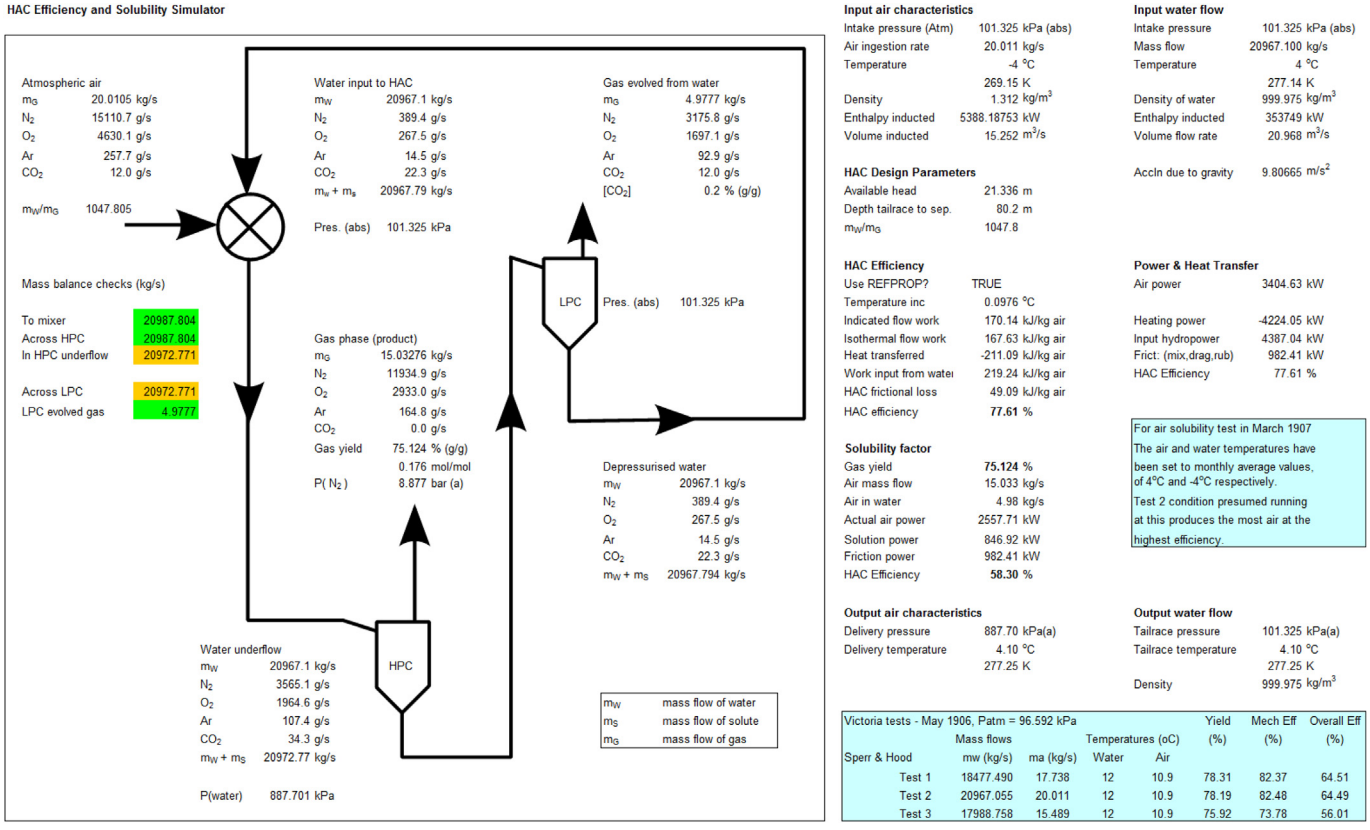

Fig. 14. Results of HAC efficiency determination for the Victoria Mine HAC for the month of March (water temperature 4 °C, air temperature −4 °C), accounting for the solubility of atmospheric gases in water. The mole fraction of oxygen in the compressed air is predicted to be 0.176. The yield of compressed air is estimated to be 75.3% (by mass). Mechanical efficiency not accounting for solubility losses is 77.36% which reduces to 58.26% when solubility losses are considered. (HPC = high pressure cyclone; LPC = low pressure cyclone).

temperature of the water would have to have been set at 6 °C, rather than 4 °C.

A second test of HAC compressed air chemical composition was undertaken using air sampled from the Ragged Chutes system, the sample being taken on 30th May, 1910. This is reported [44] as a volume proportion of oxygen also of 17.7%. The maximum daily water temperature of streams and rivers in a thermal regime close to Ragged Chutes location on the Montreal River may be estimated to be 21 °C for the 30th May 2006 [45]. Assuming this value to apply 96 years earlier, but on the same day of the year, Table 6 implies that at the time, Ragged Chutes was operating with a mass flow ratio $1350 \leq \dot{m}_W/\dot{m}_G \leq 1375$. Taylor [17] states that the rating of the Ragged Chutes compressor is 40,000 cfm FAD (18.88 m^3/s; ~22.7 kg/s @ operating temperature and pressure), and that the velocity of the two phase flow just below the mixing heads is between 4.57 m/s (15 ft/s) and 5.79 m/s (19 ft/s). Nowhere in the literature examined by this author is there a statement of the typical water flow rate required to achieve this performance, other than Langborne [5], Table 3. The mass flow ratio determined from the oxygen content of the compressed air and the river temperature (Table 6) results in a mass flow of water of 30.59 tonnes/s (30.65 m^3/s, 64,944 cfm) which should be regarded as an update of the figure of 48,000 cfm in Table 3 – which is definitely incorrect.

With the revised mass flow rate of water, under the conditions during which the compressed air sample was taken, the yield of the Ragged Chutes HAC installation is found to be 74.7% and the overall mechanical efficiency is found to be 62.2%. At 100% yield, the efficiency of the installation would be 83.3%.

The magnitudes of the compressed air loss are significant, and mean that the mass conservation elements of HAC simulation formulations, such as the one presented earlier herein, need to be modified. This is work in progress. As the solubility analyses and results presented in this section have all been based on observations of run-of-river HAC configurations, they stand irrespective of a need for an accurate numerical hydrodynamic simulator with embedded solubility physics. The mechanical efficiency of conversion of input hydropower into indicated air power is not a principal design consideration for run-of-river HAC configurations because the input energy is available at low marginal cost. However, for open or closed loop HAC configurations, the mechanical efficiency is of paramount importance because the electrical energy driving the circulation pump must be paid for.

For closed loop and open loop systems one means to mitigate that portion of the loss of efficiency that arises due to gas solubility is to consider the use of a co-solute. In general, the prior presence of a dissolved salt in water leads to reduced gas solubility; gas solubility reduces as the dissolved salt concentration increases. The Sechenov equation is commonly used for such quantitative revisions to Henry's constants [46]:

Table 5
Sensitivity of oxygen content of compressed air for the Victoria Mine HAC.

$\dot{m}_W/\dot{m}_G$	Water temp °C								
	1	2	4	6	8	12	16	20	24
900	0.178	0.179	0.180	0.181	0.182	0.184	0.186	0.187	0.189
950	0.177	0.177	0.178	0.179	0.181	0.183	0.184	0.186	0.188
1000	0.175	0.176	0.177	0.178	0.179	0.181	0.183	0.185	0.187
1050	0.174	0.174	**0.176**	**0.177**	0.178	0.180	0.182	0.184	0.186
1100	0.172	0.173	0.174	0.176	0.177	0.179	0.181	0.183	0.185
1150	0.171	0.172	0.173	0.174	0.175	0.178	0.180	0.182	0.184
1200	0.170	0.170	0.172	0.173	0.174	0.177	0.179	0.181	0.183
1250	0.168	0.169	0.170	0.172	0.173	0.175	0.178	0.180	0.182
1300	0.167	0.168	0.169	0.171	0.172	0.174	0.177	0.179	0.181
1350	0.166	0.167	0.168	0.169	0.171	0.173	0.176	0.178	0.180
1400	0.165	0.165	0.167	0.168	0.170	0.172	0.175	0.177	0.179

Table 6
Sensitivity of oxygen content of compressed air for the Ragged Chutes HAC. Green areas highlight the circumstances when an oxygen content of 0.177 mol/mol is expected.

$\dot{m}_W/\dot{m}_G$	Water temp °C								
	16	17	18	19	20	21	22	23	24
1150	0.179	0.179	0.180	0.180	0.181	0.181	0.182	0.182	0.183
1175	0.178	0.179	0.179	0.180	0.180	0.181	0.181	0.182	0.182
1200	0.178	0.178	0.179	0.179	0.180	0.180	0.181	0.181	0.182
1225	0.177	0.177	0.178	0.179	0.179	0.180	0.180	0.181	0.181
1250	0.176	0.177	0.177	0.178	0.179	0.179	0.180	0.180	0.181
1275	0.176	0.176	0.177	0.177	0.178	0.179	0.179	0.180	0.180
1300	0.175	0.176	0.176	0.177	0.177	0.178	0.179	0.179	0.180
1325	0.175	0.175	0.176	0.176	0.177	0.178	0.178	0.179	0.179
1350	0.174	0.175	0.175	0.176	0.176	0.177	0.178	0.178	0.179
1375	0.174	0.174	0.175	0.175	0.176	0.177	0.177	0.178	0.178
1400	0.173	0.174	0.174	0.175	0.175	0.176	0.177	0.177	0.178

$$\ln\left(\frac{K_{i,\text{salt}}}{K_i}\right) = k_s m \tag{5}$$

where $K_{i,\text{salt}}$ is the Henry's constant of the gas species i in the salt solution, k_s is the Sechenov coefficient, which depends on the nature of salt and solvent as well as temperature, and m is the molality (mole of dissolved salt/mass of solvent). In a 1 mol/kg aqueous solution of sodium sulphate at 25 °C, $K_{N_2,Na_2SO_4}/K_{N_2} \approx K_{O_2,Na_2SO_4}/K_{O_2} \approx 2.1$, that is, the solubility of these gases is halved. The volume of water in a closed loop HAC with a scale and (salt free) performance akin to the Ragged Chutes HAC is estimated to be 11,600 m^3. Sodium sulphate has an anhydrous formula mass of 142.04 g/mol so around 1650 tonnes of sodium sulphate would need to be dissolved in the water to bring it to a 1 molal concentration, which is a practical amount for closed or open loop systems where the liquid circulates.

For closed loop HAC systems a second means to mitigate efficiency loss due to solubility is to operate these systems at higher temperature than previously considered for run-of-river systems. As shown in Fig. 13, RHS, the higher temperature of water, the lower are the solubilities of atmospheric gases. Raising the temperature of water to 80 °C from 25 °C reduces the solubility of nitrogen gas by a factor 1.9 and that of oxygen by a factor of 2.1, that is, in terms of solubility, this has a similar effect to creating a 1 molal solution of sodium sulphate. Within a closed loop HAC, water circulating in insulated pipe work will gradually rise in temperature as a result of the heat transferred to it during the compression of the air. Such behaviour can be graphically understood from Fig. 15 which shows the transient in performance of a closed-loop version of the Ragged Chutes HAC, presumed started from ambient conditions at the beginning of the months of January (LHS) and July (RHS) and subjected to hourly diurnal air temperature variations representative of the climate of Sudbury, ON, Canada [47].

The calculations for the simulation are identical to those illustrated in Fig. 14 however the net rate of heating of the water, taken to apply throughout the hourly time interval, comprises the difference between heat added due to compression and the cooling arising from the venting of hot atmospheric gases that were formerly in solution, at the top of the riser shaft. The total heat added to a water mass of 11,600 tonnes is used to establish the starting water temperature for the next time step. When a water temperature of 80 °C is achieved, the simulation assumes a 3 MW_{th} rated, thermostatically controlled, conventional, water cooling system cuts in to maintain the temperature.

Although the simulation results of Fig. 15 cannot be taken as definitive because the model does not couple the hydrodynamics to the solubility behaviour, they are indicative of the type of transient performance that may be expected of closed-loop HACs. Starting

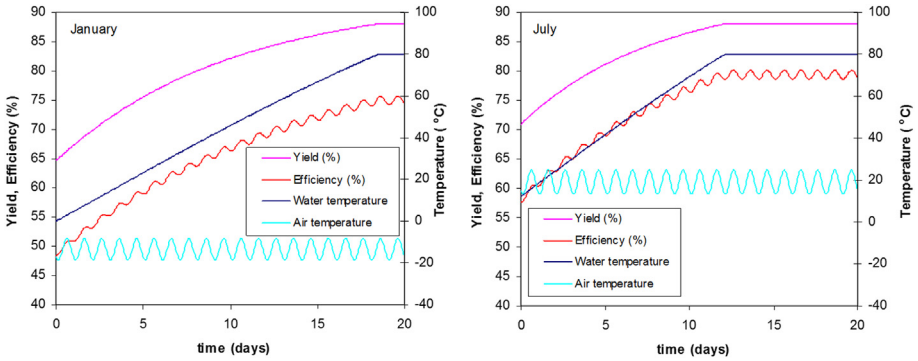

Fig. 15. Results of simulation of transient performance from ambient conditions (starting water temperature 0.1 °C for January) of a closed-loop HAC with dimensions the same as Ragged Chutes with air intake temperatures varying diurnally for January (LHS) and July (RHS) for the climate of Sudbury, ON, Canada.

the system in a January Sudbury climate does lead to self heating of the system to the thermostatically controlled temperature of 80 °C and as this occurs, the compressed air yield of the system climbs to around 87% after 18 days of operation. The mechanical efficiency climbs too, to a value of around 75%, oscillating with a diurnal pattern driven by intake air temperatures. Similar behaviour is recovered for the July simulation, but the steady-state condition is achieved after around 12 days of operation, yield remains at 87% but the overall efficiency oscillates around 80%, due to the generally higher air intake temperature. In general, the simulations indicate that the efficiency of a closed-loop HAC may be able to be manipulated by adjusting the thermostatically controlled temperature of operation, and that an 80% mechanical efficiency is not unrealistic.

7. Demonstrating the business case for HAC air compression

Given the long history of successful operations of HAC installations at the Ragged Chutes and elsewhere (Table 3), technical feasibility may not be a significant determining factor in a decision of whether or not to re-establish HAC technology in modern times. Instead, such decisions are more likely to be determined by the economics of compressed air production. The economics of closed-loop and open-loop systems, co-axial or not, clearly will be inferior to those of run-of-river or tidal HACs, as the latter exploit renewable energy at zero marginal input energy cost. However, for situations where a natural hydropower resource is unavailable, the open-loop and closed-loop systems, that incur energy input costs for pump work, may still offer significant economic advantages in comparison to modern mechanical air compressors. The reason for this is that in a HAC of any variant, the gas experiences a near isothermal compression and an isothermal gas compression process is the minimum work input compression process for any type of gas compressor [48]. Consequently, open-loop or closed-loop HACs may be regarded as energy saving, or improved energy efficiency technologies, and the modern day development determinant, is thus:

> *Do the reduced costs of energy input for an open or closed-loop HAC compensate for the capital cost of HAC installation, such that the discounted cost of compressed air delivered is lower than that of a modern day gas compressor with identical delivery performance*?

The answer to this question constitutes the core business case for modern day compression of gases using HACs, and is reported in the forthcoming discussion.

The techno-economic analysis undertaken to assess the business case for HAC air compression comprised two main components: i) estimation of the technical performance of a contemporary compressor and a HAC plant meeting the same duty and ii) discounted cash flow modelling of the modern and HAC installations.

For the contemporary plant, a three stage centrifugal compressor system was assumed with intercoolers and an aftercooler, with equal pressure ratios for each of the 3 stages, the same overall pressure ratio and the same free air delivery (FAD) as for the HAC plant. The technical and economic performance of this plant was compared to:

i) A closed loop HAC with identical layout and performance as the Ragged Chutes installation but with the compression power required being supplied by a circulation pump. On the basis of prior discussions, a mechanical efficiency of 83% for Ragged Chutes, was adopted. This reflects the ratio of useful air compression power to the magnitude of the natural hydropower resource, with the balance being used to overcome the frictional, bubble drag and minor losses present within the system. The rating of the equivalent circulation pump was thus obtained through calculation of the compression power for a duty approximating that for Ragged Chutes (FAD 18.9 m^3/s, pressure ratio = 9) and dividing this value by the product of the HAC efficiency and an electric motor efficiency assumed at 95%.
ii) A closed loop HAC also using a circulation pump, but utilizing an underground structure at depth that forms a water–air separation cyclone, such as that of [49] or as described and analysed in detail by Wang [38]. The effect of this is that the capital cost of developing a 300 m long, 8 m high, 6 m wide air separation chamber (~CAD 4 million in 2013 terms) is avoided, and the capital cost of a cyclone separator chamber of dimensions 10 m in height and 20 m in diameter is introduced.
iii) A run-of-river HAC identical to the Ragged Chutes installation, utilizing a natural hydropower resource.
iv) A run-of-river HAC utilizing a natural hydropower resource, but equipped with a cyclonic separation chamber, identical to that for case ii).

For the centrifugal compressor, the isentropic exponent was taken as 1.4, the isentropic efficiency of each stage was assumed to be 80% and the electric motor efficiency was assumed to be 95%. Given intake air conditions of 100 kPa and 15 °C, and a specified delivery pressure, the isentropic compression work for each stage was calculated, the isentropic and motor efficiencies were applied, and the electric motor power required of each stage (approximately equal) was totalled.

Table 7 presents the results of the technical analysis. It shows that as the pressure ratio increases, the percentage reduction in electric motor installed capacity increases, in favour of the HAC.

Essentially, this percentage measures the extent of deviation of the 3 stage centrifugal compressor system process lines from an isothermal compression process line, to a given delivery pressure. A HAC delivers a near isothermal compression process. For a delivery pressure of 9 bar, the electric motor driving the circulation pump in a closed loop HAC would be rated at 5.3 MW, 13.5% lower than the 6.1 MW rated centrifugal compressor motor. If the centrifugal compressor was single stage, its compression process would deviate significantly from isothermal and it would have a rating of 7.6 MW (the HAC pump motor rating would be 38.5% lower).

The economic system analysis was conducted from the point of view of the owners of a new 'for-profit' corporation, based in the mining district of Sudbury, in Northern Ontario, Canada. The business of this new corporation would be the supply of large volumes (18.9 m^3/s) of compressed air at a supply pressure of 9 bar, either for a collective of mines (as was the case for Ragged Chutes at Cobalt) or for a large, centralised compressed air consumer such as an oxygen plant. The analysis was based on identifying whether to opt for a 3 stage centrifugal compressor (now abbreviated to '3SCC') to produce the compressed air, or to choose to install a HAC.

For either the 3SCC or the HAC, the design operating life was assumed to be 9 years. While a rather short life for an HAC given the experience at Ragged Chutes, 10 years is fairly typical for the design life of a centrifugal compressor (or the time between major overhauls). For both the 3SCC and the HAC there is a risk that the demand for the air will move away, if reserves of ore become depleted or diminished due to a significant fall in the mines' commodity price.

The Canadian federal tax rate was set at 15% and the Ontario provincial tax rate was set at 11.5%. Capital allowances were computed on a straight-line basis, starting in the second year of the project life, to year 10. Tax was assumed paid in the year the liability was incurred. Working capital, assumed first incurred during the first year of production, was taken to be equivalent to 3 months operating costs. This was assumed recovered in the year after compressed air production ceased.

As a business concern, the corporation would sell compressed air to its customers, at a price expressed in terms of CAD (2013 basis)/tonne. For purposes of computing revenues realizable by either 3SCC or HAC projects, the performance of an Atlas Copco GT153 system was analysed to form a suitable benchmark for comparison, as the technical performance of this equipment could be estimated and a recent procurement cost for such equipment was available in the public domain [35]. Being the largest ever supplied by the world's largest air compressor manufacturer, the sale price of compressed air established for this plant can be considered to be an estimate of the lowest sale price for compressed air attainable at the present time. Assuming that the business held the capital to finance the project (i.e. equity only), the sale price for compressed air would not only depend on the procurement price, but also on:

- its cost of installation (assumed to be 6% of its procurement cost [50]),
- its maintenance cost (assumed to be 3.8% of procurement cost per annum, further assumed to exclude labour [50]),
- the cost of manning the plant (assumed to be 6 operatives, working shifts with an average salary of CAD 80,000 per annum)
- the cost price of electricity
- the cost of capital for the plant operator

At the time of writing, the lowest cost of electricity procurable by an industrial consumer operating in Northern Ontario is represented by the value of CAD 55/MWh (2013) in Table 8. Very large consumers may be able to obtain an electricity procurement (cost) price of CAD 65/MWh with all available incentives and benefits being secured, but this could range up to CAD 80/MWh for those who have not secured, or who are unable to secure, such benefits. The cost of capital (return rate) depends on the level of risk associated with the venture, as perceived by the businesses investors. The values in Table 8 reflect a very large scale, modern air compressor with 80% efficiency that may be interpreted as floors for the compressed air sale price exploiting all economies of scale. As such, they may be used to inform interpretation of the results of discounted cash flow modelling of the respective 3SCC and HAC project options. However, it should be noted that, in terms of production scale, the FAD of Ragged Chutes is approximately one fifth of that of the GT153 system.

To support the analysis, costs of procurement of an 18.9 m^3/s FAD, 9 bar, 3 stage centrifugal compressor were obtained from a well-known manufacturer. These amounted to CAD 1 million for the compressor and CAD 0.2 million for its cooling pack. Installation, maintenance, labour and other costs were estimated as described previously. Application of the so-called 'six-tenth rule' to downscale the installed cost for the Atlas Copco GT153 produced a total of CAD 3.9 million, sufficiently different from the installed cost of CAD 1.2 million (using the procurement costs from the well-known manufacturer) to carry this higher cost forward into the analysis as a separate scenario.

Costs for installation of a Ragged Chutes replica to produce 18.9 m^3/s FAD at 9 bar were obtained from a well established mine construction company furnished with the drawing in Fig. 9 and other design details. The costs can be summarised as follows:

- Downcomer Shaft: CAD 1.3 million (Blind sink, 110 m deep, 3.0 m finished diameter, concrete lined, 4.2 m excavated diameter)

Table 7
Estimated installed rating of electric motors for a 3 stage centrifugal compressor (3-Stage CC) and a HAC using a circulation pump (in closed loop systems), for varying delivery pressure and FAD 18.9 m^3/s.

Pressure ratio	Motor rating (kW)		HAC % lower
	3-Stage CC	HAC @ 83%	cf 3-Stage CC
2	1781.9	1661.2	6.8
3	2880.2	2632.5	8.6
4	3685.6	3321.4	9.9
5	4325.7	3855.5	10.9
6	4859.0	4291.8	11.7
7	5317.2	4660.5	12.4
8	5719.7	4979.7	12.9
9	6079.0	5261.2	13.5
10	6403.9	5513.0	13.9
15	7686.0	6480.7	15.7

Table 8
Estimated break-even sale price of compressed air (2013 CAD/tonne) produced from an Atlas Copco GT153 multi-stage, centrifugal compressor installed and operating in Sudbury, Ontario, for a range of return rates and a range of electricity procurement prices.

Cost of capital (%)	Electricity price (2013 CAD/MWh)			
	55	65	70	80
2	3.984	4.596	4.902	5.514
5	4.108	4.726	5.035	5.653
10	4.331	4.958	5.271	5.898
15	4.574	5.210	5.527	6.162
20	4.839	5.482	5.803	6.445

- Separation Gallery: CAD 4.0 million (Drill & blast, 300 m long, 8 m × 6 m section, 5 m cable bolts on 3 × 3 m pattern, shotcreted floor, roof and walls to 0.076 m thickness)
- Riser Shaft: CAD 1.2 million (Raise bored shaft, 100 m deep, 3.0 m fished diameter, concrete lined, 3.5 m excavated diameter)

The total capital costs allowed for a further CAD 1.0 million for balance of plant items, in addition to the construction cost total of CAD 6.5 million. For scenarios involving replacement of the 300 m long separation gallery with a cyclonic chamber, the construction costs were lowered by CAD 3.0 million.

For all HAC scenarios, the historical record for Ragged Chutes motivated a cost of CAD 0.00/annum for maintenance (2 shutdowns in 70 years, no moving parts). One operative for each of 3 shifts were assumed to be employed at an average rate of $80,000 per annum. Installation of a HAC to opportunistically utilize a natural hydropower resource was considered as a technology scenario (exactly as at Ragged Chutes, and in these cases, electricity consumption was set to zero).

The observations that can be made of Table 9 are as follows:

1) At a compressed air sale price of CAD 4.958/MWh, the only economically viable multi-stage centrifugal compressor solution is the Atlas Copco GT153, and this is only for a cost of capital lower than 10%. However, note that in Table 9, this plant is supplying ~5 times higher FAD and 2/3 of the delivery pressure than the other options. Furthermore, the scale of the FAD is such that it may approximate the total demand of all mineral production operations in Sudbury, including smelters. Not all of the air produced by this plant could be sold, but the results in Table 9 assume that it can be; the GT153 entries are present only to provide a reference benchmark at very large scale. Thus the HAC with or without cyclonic chamber but both using a natural hydropower resource (if available) is the only practical option for supply of compressed air assessed in terms of the NPV returned at all discount rates considered. (<17.5% for the Ragged Chutes replica).
2) At a compressed air sale price of CAD 5.482/MWh an Atlas Copco GT153 could support a return rate of 20%, if all its air could be sold. A closed-loop HAC with cyclonic chamber could be viable if capital could be secured at public sector rates (assumed to be 2%). The HAC with or without cyclonic chamber, but both using a natural hydropower resource (if available), is the only practical option for supply of compressed air.
3) At a compressed air sale price of CAD 6.000/MWh, the 3SCC may be feasible at costs of capital lower than ~8%, if these manufacturer's capital cost quotes are to be believed. The closed-loop HAC with cyclonic chamber returns superior NPV at the same costs of capital and thus would be preferred if a natural hydropower resource was not available. The natural hydro powered HAC with or without cyclonic chamber remains the best option.
4) At a compressed air sale price of CAD 7.000/MWh the 3SCC with Manufacturer's capital cost estimates returns positive NPV up to a discount rate of 20%. The 3SCC with capital cost scaled down from the GT153, using the sixth-tenths rule, becomes feasible with a cost of capital at or below 10%. The closed-loop HACs without or with cyclonic chamber offer higher NPV, for costs of capital at or below 20% for the latter option, and are thus preferred.
5) At a compressed air sale price of CAD 8.000/MWh the 3SCC, with capital costs estimated by scaling down from the GT153 with the sixth-tenths rule, becomes a feasible option for all discount rates considered. Across the same range of discount rates, the closed-loop HAC with cyclonic chamber is preferred on the basis that it returns higher NPV. At a discount rate ~13% or below, the closed-loop HAC without cyclonic chamber is preferred over 3SCC via six-tenths, although the closed-loop HAC with cyclonic chamber would be preferred over both. If a natural hydropower resource is available, hydro powered HACs with or without cyclonic chamber offer far superior economic performance across all costs of capital.

In short, the results of the techno-economic analysis support the notion that there is not one of the compressed air sale price scenarios explored where an HAC solution is found to be inferior to a 3SCC solution.

8. Potential modern applications of HACs

A cheap and reliable supply of compressed air is still of very high value for modern mining practice. HAC System X (Fig. 7) would deliver just under 10,000 cfm free air at 9.8 bar absolute (128 psi gauge).

HACs are of interest at present for new application areas, and the dominant reported interest appears to be in the field of coupling HACs to gas turbines [51–54] for power generation, so that Brayton cycle systems can benefit from isothermal compression. HACs for compressed air storage also seem an obvious application area [55]. Other than the obvious provision of compressed air, contemporary mining practice offers additional niche opportunities for HACs, motivated by potential cost reductions, reduced primary energy consumption or reduced CO_2 emissions. Some suggested new applications, motivated by a lower cost for compressed air are discussed in the following.

8.1. Deep mine ventilation air cooling

Deep mining operations, such as the base metal mines of Northern Ontario or precious metal mines of the Republic of South Africa face significant technical and cost challenges in the refrigeration of mine ventilation air. Hydraulic compressors are cited as a potential new technology for cooling by Fischer et al. [56] in their comprehensive 1994 assessment and by Brown and Domanski [57] in their 2014 update of viable alternative cooling technologies, but both sets of authors consider only the compression of CFC and HCFC vapours within falling columns of water as part of a conventional vapour compression refrigeration scheme, and fail to recognise the integrated benefits of dehumidification and pressure boosting obtainable by adopting air as the working fluid. As indicated in Fig. 16, using the compressed air from HAC System X in an ideal device that could expand the air isentropically (while producing work!) would produce a 3.8 kg/s stream of −126.1 °C compressed air with a cooling power of (419.14−271.94) kJ/kg × 3.8 kg/s = 560 kW_{th}, deliverable to the bulk mine ventilation air (20-21-22, in Fig. 6) through the direct contact of mixing, 17-18-21 in Fig. 6. This is sufficient cooling power to reduce a shaft bottom ventilation inflow of 800 m^3/s (1,695,120 cfm) by 0.58 °C which is of economic significance.

For large pressure ratios, compressed air produced by a HAC is drier than mechanically compressed atmospheric air [58]. To illustrate, the psychrometric properties of air are such that for HAC System X, air at 9.8 bar with a dry bulb temperature of 10 °C that is saturated (wet bulb temperature 10 °C) has a saturation moisture content of 0.78 g H_2O/kg of dry air. These are the conditions of the compressed air that would be expected at the base of the downcomer shaft just before it is separated. In contrast, mechanically compressed air retains the moisture content of the air at the point of intake to the compressor throughout its compression process. Supposing atmospheric air at 10 °C dry bulb and 60% relative

Table 9
Net Present Values for compressed air price, discount rate and technology option scenarios for an electricity procurement price of CAD 65/MWh. Green areas = viable; yellow areas = not viable (2013 prices).

Electricity price		65 CAD/MWh	Compressed air price			4.958 CAD/tonne
Technology scenario	CAPEX	NPV (million CAD, 2013) at discount rate				
	(million CAD)	2%	5%	10%	15%	20%
Atlas Copco GT153	10.1	7.31	3.96	0.00	-2.64	-4.44
3 stage centrifugal CIM	1.3	-4.75	-4.40	-3.90	-3.51	-3.20
3 stage centrifugal 6th10ths	**3.9**	**-8.22**	**-7.73**	**-7.07**	**-6.56**	**-6.16**
Closed loop HAC	7.5	-4.99	-5.51	-6.10	-6.48	-6.72
Closed loop HAC with Cyclone	4.5	-2.00	-2.52	-3.13	-3.51	-3.77
Hydropower HAC	7.5	8.30	5.88	2.87	0.75	-0.78
Hydropower HAC with Cyclone	4.5	10.58	8.26	5.38	3.35	1.87

Electricity price		65 CAD/MWh	Compressed air price			5.482 CAD/tonne
Technology scenario	CAPEX	NPV (million CAD, 2013) at discount rate				
	(million CAD)	2%	5%	10%	15%	20%
Atlas Copco GT153	10.1	17.88	12.91	6.92	2.85	0.00
3 stage centrifugal CIM	1.3	-1.78	-1.89	-1.96	-1.97	-1.95
3 stage centrifugal 6th10ths	**3.9**	**-5.25**	**-5.22**	**-5.13**	**-5.02**	**-4.91**
Closed loop HAC	7.5	-2.03	-3.00	-4.16	-4.94	-5.48
Closed loop HAC with Cyclone	4.5	0.55	-0.37	-1.46	-2.19	-2.70
Hydropower HAC	7.5	9.93	7.26	3.94	1.60	-0.09
Hydropower HAC with Cyclone	4.5	12.22	9.64	6.45	4.19	2.56

Electricity price		65 CAD/MWh	Compressed air price			6.000 CAD/tonne
Technology scenario	CAPEX	NPV (million CAD, 2013) at discount rate				
	(million CAD)	2%	5%	10%	15%	20%
Atlas Copco GT153	10.1	28.35	21.76	13.77	8.28	4.39
3 stage centrifugal CIM	1.3	0.96	0.42	-0.19	-0.57	-0.82
3 stage centrifugal 6th10ths	**3.9**	**-2.32**	**-2.74**	**-3.21**	**-3.50**	**-3.68**
Closed loop HAC	7.5	0.42	-0.93	-2.56	-3.67	-4.45
Closed loop HAC with Cyclone	4.5	2.71	1.46	-0.05	-1.08	-1.80
Hydropower HAC	7.5	11.54	8.62	4.99	2.44	0.58
Hydropower HAC with Cyclone	4.5	13.83	11.01	7.50	5.03	3.24

Electricity price		65 CAD/MWh	Compressed air price			7.000 CAD/tonne
Technology scenario	CAPEX	NPV (million CAD, 2013) at discount rate				
	(million CAD)	2%	5%	10%	15%	20%
Atlas Copco GT153	10.1	48.54	38.85	26.98	18.75	12.87
3 stage centrifugal CIM	1.3	5.16	3.97	2.56	1.60	0.93
3 stage centrifugal 6th10ths	**3.9**	**2.53**	**1.35**	**-0.06**	**-1.02**	**-1.67**
Closed loop HAC	7.5	4.58	2.59	0.17	-1.51	-2.70
Closed loop HAC with Cyclone	4.5	6.87	4.98	2.68	1.08	-0.05
Hydropower HAC	7.5	14.66	11.25	7.03	4.05	1.89
Hydropower HAC with Cyclone	4.5	16.94	13.64	9.54	6.64	4.54

Electricity price		65 CAD/MWh	Compressed air price			8.000 CAD/tonne
Technology scenario	CAPEX	NPV (million CAD, 2013) at discount rate				
	(million CAD)	2%	5%	10%	15%	20%
Atlas Copco GT153	10.1	68.74	55.93	40.19	29.22	21.35
3 stage centrifugal CIM	1.3	9.32	7.49	5.28	3.76	2.68
3 stage centrifugal 6th10ths	**3.9**	**6.69**	**4.87**	**2.66**	**1.14**	**0.07**
Closed loop HAC	7.5	8.74	6.11	2.89	0.65	-0.96
Closed loop HAC with Cyclone	4.5	11.03	8.50	5.40	3.24	1.70
Hydropower HAC	7.5	17.77	13.89	9.07	5.66	3.20
Hydropower HAC with Cyclone	4.5	20.06	16.28	11.58	8.26	5.85

humidity (rather low) is drawn into a mechanical compressor, its moisture content is then 4.57 g H_2O/kg of dry air, substantially higher than the 0.78 H_2O/kg of dry air of the HAC alternative. The importance of these distinctions is that mixing of compressed air from HAC System X with the bulk mine ventilation air would result in drier mine ventilation air. As the main mode of cooling for humans working in the subsurface is evaporative cooling, lowering of the wet bulb temperature of the mine ventilation air delivered to the workings provides the air with greater effective cooling capacity.

Where deeper mining is being carried out, it is possible that greater depths of HAC can be entertained, such as HAC System Y of Fig. 8, which operates at 600 m depth. 11.2 kg/s air at 56 bar gauge could be produced by such a system (assuming nil dissolved

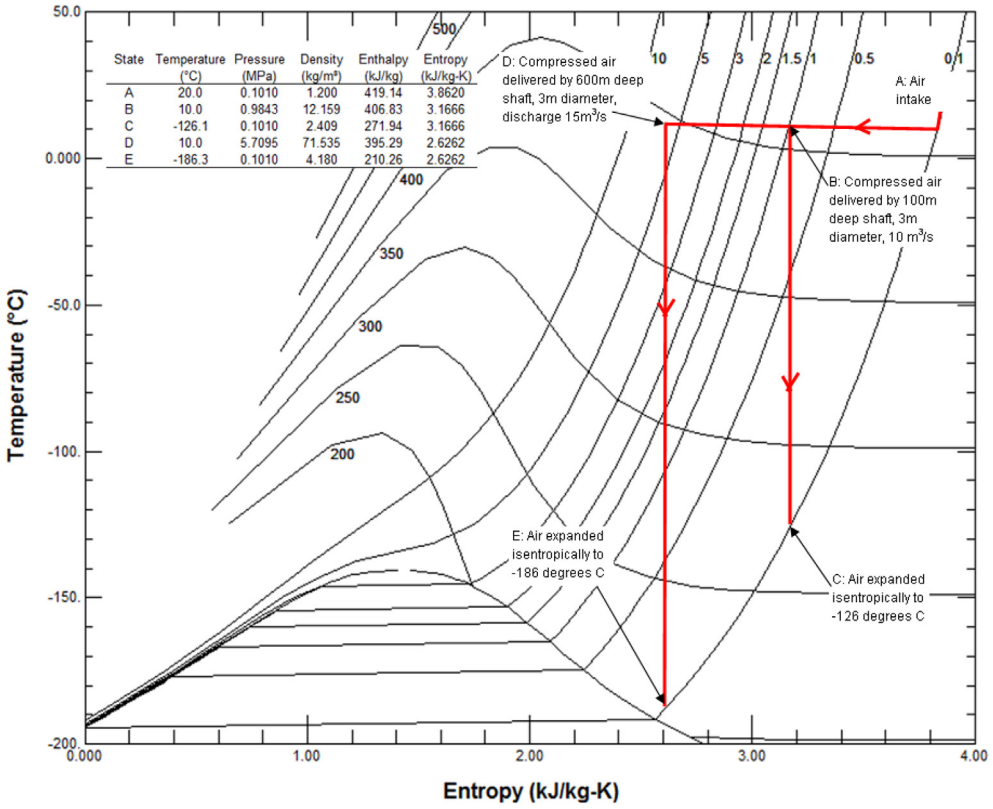

Fig. 16. Temperature-entropy (T–S) diagram for air showing states of compressed and decompressed air from HAC simulations of Fig. 7 and 8.

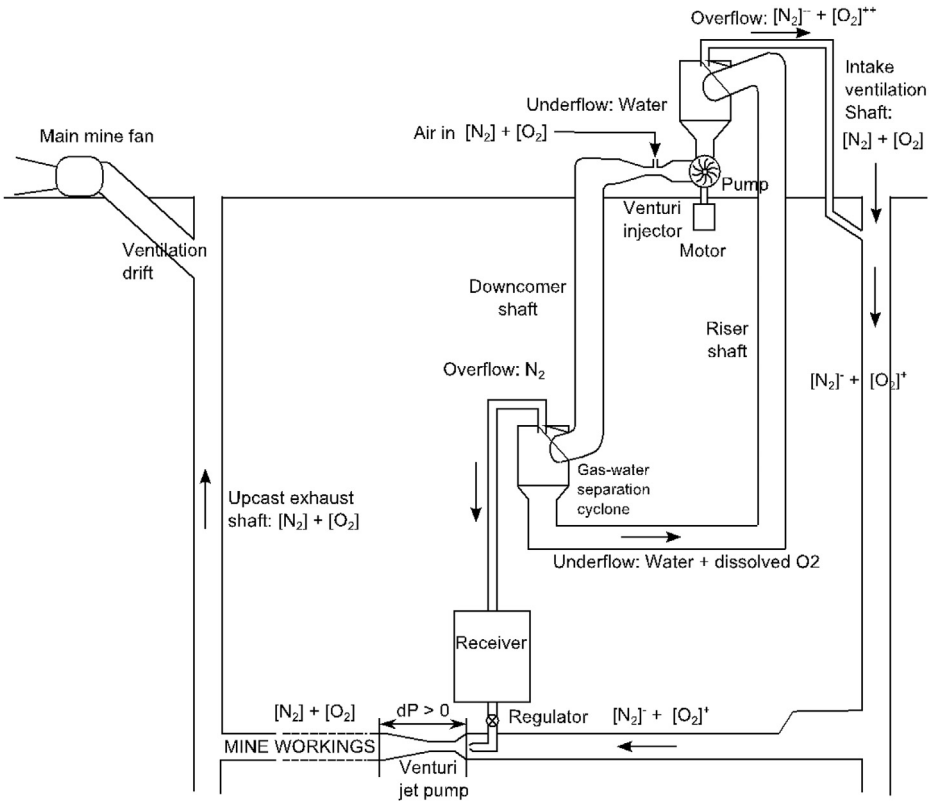

Fig. 17. Schematic of a closed loop HAC operated with a circulation pump for mine ventilation air cooling, dehumidification and pressure boosting. $[X]^{+}$ = enrichment of species X; $[Y]^{--}$ = significant depletion of Y.

gases—which would inevitably occur, but could be mitigated with co-solutes or high operating temperatures), that, if expanded isentropically could cool a shaft bottom air flow of 800 m^3/s by 2.4 °C. Importantly, as well as cooling the air, the high velocity jet issuing from Station 18 (Fig. 6)would tend to entrain the surrounding, much lower velocity, bulk mine ventilation air, increasing the velocity of the latter. Assuming the jet becomes completely mixed with the bulk ventilation air by Station 21, profiling the airway 21 to 22 such that it is divergent with an angle no greater than 17° each side of the tunnel axis (to avoid flow separation), the increase in kinetic energy of the bulk mine ventilation air flow caused by the jet can be converted into pressure energy, that is, the pressure of the air would increase between 21 and 22 (Fig. 6).

The combined effect of the jet on the bulk mine ventilation air is akin to an integrated air cooler, dehumidifier and booster fan. The concept is illustrated in Fig. 17. For pressures of 56 bar gauge (depths of 600 m), uncoupled solubility calculations that ignore solution kinetics, indicate that oxygen solution may be complete, meaning that any refrigerating and pressurising effect, 17-18-21-22 of Fig. 6, may be attributable only to nitrogen. In Fig. 17 the high pressure cyclonic separator is at such a depth that the oxygen of the inducted air is assumed completely dissolved and only nitrogen gas needs to be separated from the water. Dissolved oxygen gas would come out of solution at the top of the riser shaft (15 of Fig. 6) and can be captured in a canopy above the riser stilling tank, or forcibly separated from water with a low pressure cyclone (Fig. 17). A small suction pressure arising from a connection between the overflow of such a cyclone and the ventilation air intake shaft (in an exhausting system), would ensure that this oxygen would then enrich the bulk ventilation air. Low pressure cyclone underflow will be water with the oxygen and nitrogen solubilities identical to intake conditions, which passes to the circulation pump. Make up air is shown drawn into the closed loop HAC for compression by means of a venturi injector. At depth, high pressure nitrogen gas passes to a venturi jet pump arrangement that will cool and dehumidify the bulk, oxygen enriched, autocompressed mine ventilation air entering the level via the intake downcast shaft and boost its pressure.

8.2. *A speculation on a future for hydraulic gas compressors: carbon capture from fossil fuelled plant*

The differential pressure solubility of gaseous species in water may also present an opportunity for cost effective gas separation using hydraulic gas compressors (HGC), a generalization of HACs. Combustion gases from fossil fuelled plant using air (boilers, electricity generating stations, furnaces, etc.) predominantly comprise CO_2, water vapour, and N_2, with much smaller concentrations of undesirable species such as NO_x, SO_2, and possibly unburned hydrocarbons, or O_2—if the plant operated with significant excess air. For simplicity in explanation of the following conceptual outline, it is assumed that the combustion gas comprises only: CO_2, H_2O and N_2.

When the combustion gas bubbles come into contact with the water in the downcomer shaft, the water vapour will condense into the water readily (if the water has not already become condensate prior to being passed to the HGC as part of a heat recovery scheme). This will leave a stream of gas bubbles with a composition of CO_2 and N_2.

It is evident from Fig. 13 that CO_2 has pressure solubility in water at least an order of magnitude higher than N_2 and thus CO_2 will dissolve more readily in the water as the pressure increases. Fig. 18 shows the expected compositions of exhaust gas bubbles in large scale HGCs, taken to be coupled to 40 MW_e rated fossil fuelled electricity generating plants, each utilizing a different fossil fuel. The methane (gross calorific value = 55.5 MJ/kg) fuelled plant is taken to be gas engine based with a heat recovery steam generator to a second cycle, with an overall efficiency of 45%. The diesel and anthracite fuelled plants have lower rated capacities implied as their efficiencies will be lower, but the same mass flow of exhaust gas is assumed for the solubility simulations of Fig. 18. At zero equivalent metres H_2O, the different mole fractions at input are a result of differing combustion chemistries, but with each chemistry assuming stoichiometric proportions of oxygen in air. The curves for the CO_2 species indicate near complete solubility dictated by the partial pressure of nitrogen only at a pressure of >65 m H_2O, and similar qualitative behaviour across the three fuels. The water mass flow rates used in preparation of Fig. 18 are 22,700 kg/s, roughly matching that of the Ragged Chutes installation at Cobalt and thus suggest that an HGC installation of that scale could capture the CO_2 emitted by a 40MW_e rated cogeneration plant, burning gas.

Fig. 19 shows a schematic of the concept comprising a single HGC coupled to a fossil fuelled power station. As the water and admitted exhaust gas descend in the downcomer, the CO_2, as the most soluble species of the gas mixture, dissolves readily, for the most part being partitioned to the water phase, with CO_2 concentration in the gas phase significantly diminished. Separating the

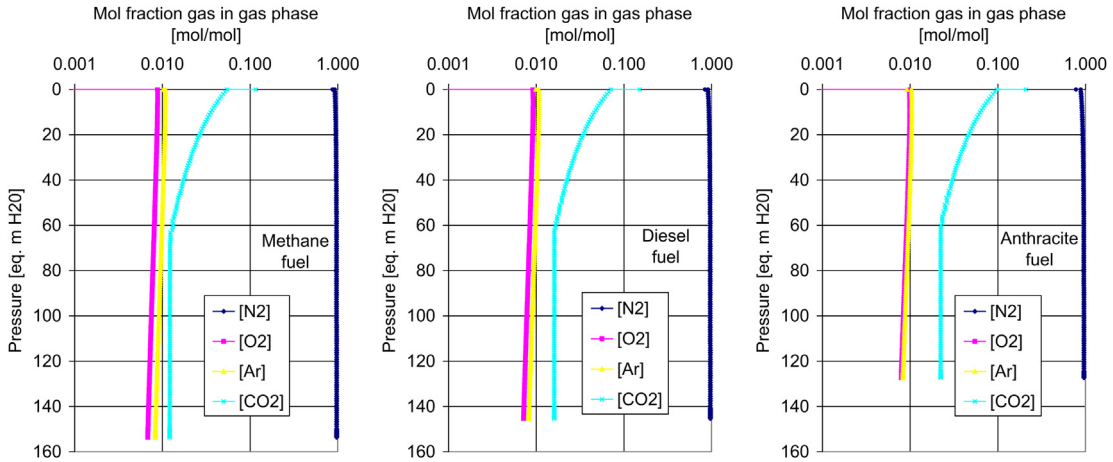

Fig. 18. Gas solubility profiles for a HAC with water flow rate 22,700 kg/s and exhaust gas flow rate 25.505 kg/s. The composition of exhaust gas for methane fuel (LHS) is: CO_2 0.117069, N_2 0.872654, Ar 0.010277, O_2 0.00001 mol/mol; for diesel fuel (Centre) is: CO_2 0.152024, N_2 0.838106, Ar 0.009870, O_2 0.00001 mol/mol and for anthracite fuel is: CO_2 0.209600, N_2 0.781200, Ar 0.009200, O_2 0.00001 mol/mol. For the methane plant, the mass flow of methane is 1.60 kg/s corresponding to a heating rating of 88.6MW_{th} and a net power output of 40 MW_e. The water mass flow rate matches that of the Ragged Chutes installation at Cobalt, Ontario.

water from the gaseous phase with a high pressure cyclone, effectively separates the CO_2 from the N_2, which is taken to mean a selective capture of the CO_2. As the water depressurises while it ascends, gas solutes previously dissolved in the water become less soluble and will come out of solution to create a new gaseous phase. At the top of the riser, the flow will be two phase and so the gas stream can be separated from the water with another (low pressure) cyclone.

The purpose of a second HGC system cascading from the first is to increase the purity of the CO_2 stream. In Fig. 20, each HGC system comprises: an inlet mixer, a downcomer shaft, a high pressure cyclone (HPC) gas–liquid separator, a riser shaft and a low pressure cyclone (LPC) gas–liquid separator. The riser depths of the cascaded HGCs are not identical. The first (100 m riser depth) has been set to match the Ragged Chutes situation so that its performance as a carbon capture device could be assessed (it could handle emissions from a $40MW_e$ rated cogeneration plant). The second (52 m riser depth) has been adjusted to improve the purity of the nitrogen and carbon streams.

The mass balances (Fig. 20) arising from the solubility calculations show that the first HGC captures 92.8% of the CO_2 entering the system as gas dissolved in the water and produces a 17.1 kg/s stream of nitrogen at 10.8 bar with 96% (g/g) purity. When dissolved gases come out of solution as the water passes up the riser shaft, a stream of 8.5 kg/s gas is produced where the CO_2 concentration is 47.6% (g/g), potentially too low for economic application. To enhance the CO_2 purity, this stream passes to the second, cascaded, HGC that ultimately produces a 4.7 kg/s stream of CO_2

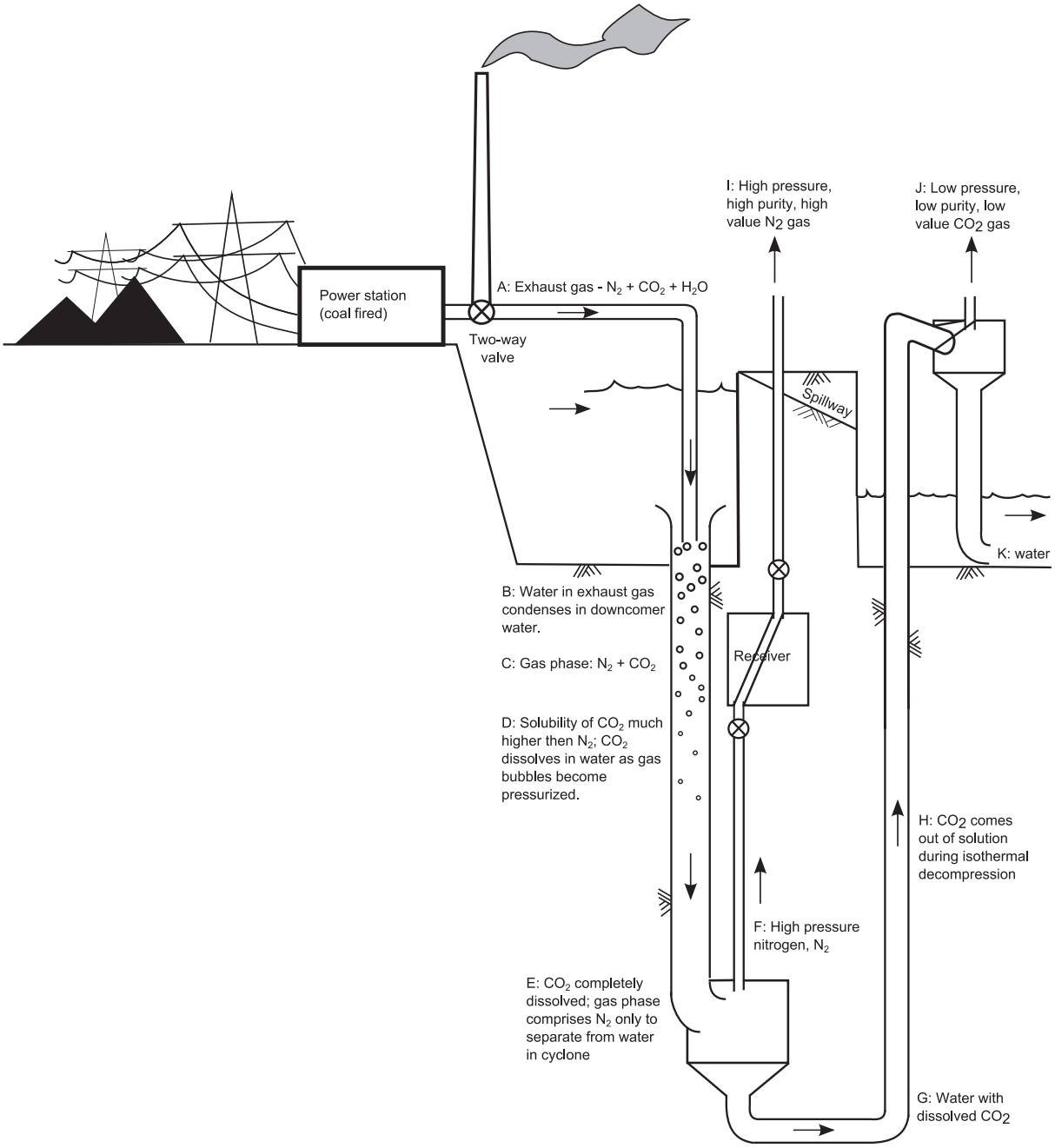

Fig. 19. Schematic of a hydropower driven HGC for CO_2 capture from a fossil fuelled electricity generating station, and co-production of a commercially valuable high pressure stream of N_2 gas.

with 83.3% (g/g) purity and a second stream of 3.9 kg/s nitrogen with 93% (g/g) purity at 6.1 bar.

Overall 89.9% of the CO_2 admitted to the system is separated (captured) and could pass to further processes for sequestration. If the power plant ran with a load factor of 80%, the total CO_2 captured would amount to 0.110 million tonnes per annum.

When additional gas species are considered in the system, such as O_2, which may be present due to the combustion process taking place in excess air, whether or not these species predominantly arrive at the high pressure overflow or the low pressure overflow depends on their relative pressure solubility.

Run-of-river HGCs are assumed in this gas separation application. Despite their vertical extents, HACs utilizing natural hydropower resources need not be high head devices and can be designed to operate with very low head (2 or 3 m), as may be available close to a river, or at a coastline with a macrotidal regime. The requirement for an opportunistically available natural hydropower resource is not strong for this carbon capture application of HGCs. The reason for this is that the majority of coal fired electricity generating stations adopt variations of the Rankine power cycle, meaning that large amounts of cooling water are required to condense steam on the low pressure side of the stream turbines of those systems. Consequently coal fired power stations tend to be located close to rivers inland or at the coast, where these large volumes of water are available and there may thus be appreciable potential for HAC deployment for carbon capture uses.

9. Conclusions

This paper has reviewed some of the reported reasons for the demise of HACs, most or all of which are surmountable, or of little relevance, in modern mining practice. Where there are sources of head, HAC installation developed down to ~100 m depth may thus still be able to make significant contributions to energy savings and thus production cost reductions in mining operations.

The principle of system operation of a HAC exploiting a hydropower resource has been explained. HACs should be designed so that the hydropower resource can be optimally exploited by regulating the water discharge, for given conditions of head.

An outline of an updated formulation for HAC performance simulation was presented, which provides a modest advance on models published elsewhere because the initial relative velocity of the gas phase bubbles is computed. The values obtained were found to agree well with the experimentally established value adopted by other workers.

The modern taxonomy of HACs presented evolutions of Taylor's original designs of HACs to produce solutions that would be applicable to situations were no natural hydropower resource is available. There is precedent from one of Taylor's designs and practices in the oil and gas industry, for the use of cyclonic water-gas separation systems.

Although the solubility computation results presented herein were not coupled to the hydrodynamical formulation, the predictions of the mole fraction of oxygen remaining in the gaseous phase agreed closely with observations taken, historically, at the Victoria Mine and Ragged Chutes HAC installations. Estimation of the mechanical efficiency of HACs required consideration of a so-called 'nearly isothermal' process for the water, so that the small water temperature rise due to the compression heat could be estimated, and a polytropic process for the air from inlet to outlet, but near isothermal during the actual compression. Applications of HACs with deeper shafts for open-loop or closed-loop systems may be feasible but will require investigation of viable co-solutes to minimise compressed air loss due to gas solution or investigation of

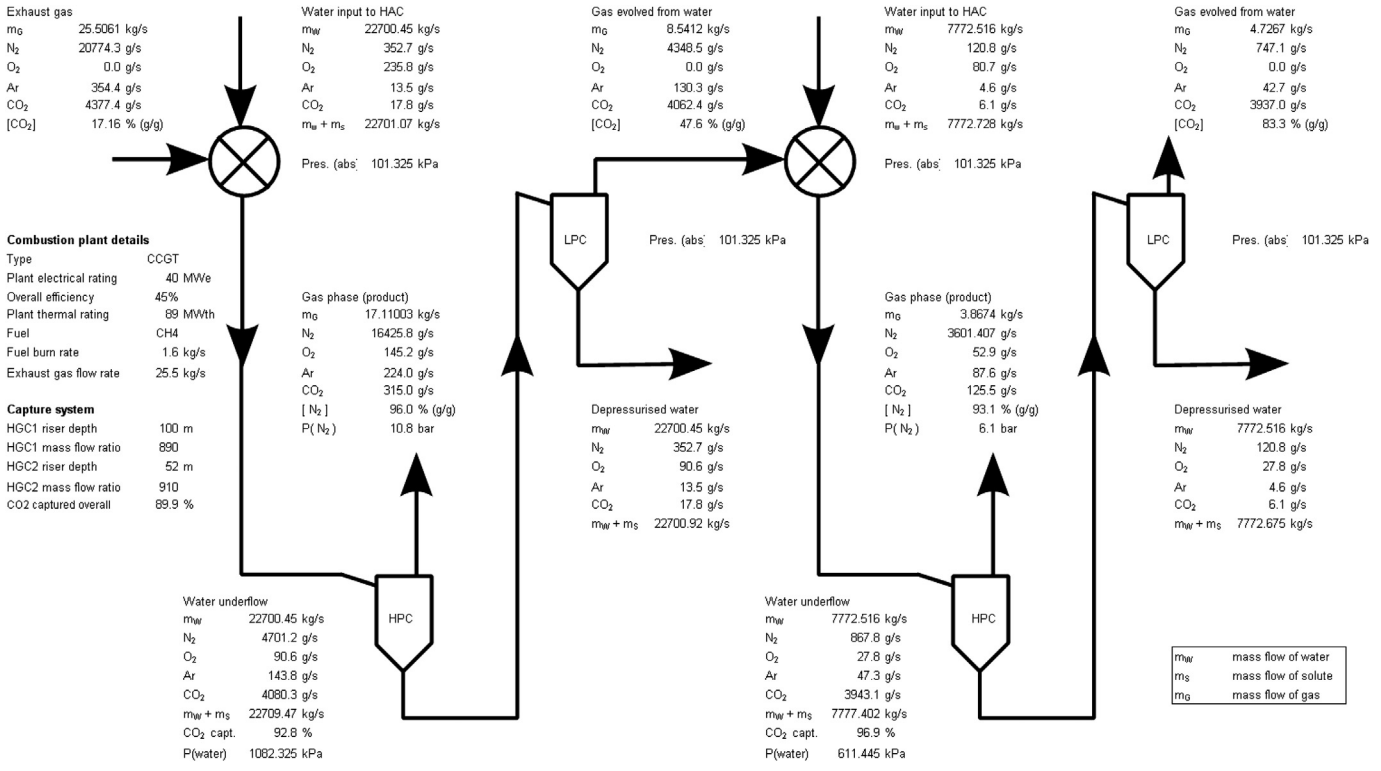

Fig. 20. A schematic of a cascaded HGC system for carbon capture from a fossil fuel electricity generating plant rated at 40MW_e fuelled by methane. The first HGC captures 92.8% of the CO_2 entering the system as gas dissolved in the water and produces 17.1 kg/s stream of nitrogen with 96% purity. When dissolved gases come out of solution as the water passes along the riser shaft, a stream of 8.5 kg/s gas is produced, where the CO_2 concentration is 47.6%, potentially too low for economic application. To enhance the CO_2 purity, this stream passes to a second, cascaded, HGC that ultimately produces a 4.7 kg/s stream of CO_2 with 83.3% purity and a second stream of 3.9 kg/s nitrogen with 93% purity.

high temperature operation of HACs. Either of these mitigation measures reduce gas solubility and hence may be expected to increase the yield of compressed air and hence the mechanical efficiency. Simulations of transient performance of closed-loop HACs indicated that the yield and mechanical efficiency may be chosen by means thermostatic control of the circulating water temperature.

A techno-economic analysis of HACs deployed for the production of compressed air at FAD volumes and delivery pressures useful for mineral production revealed that either closed-loop HACs, that solely utilize the nearly isothermal compression characteristic, or HACs that opportunistically utilize natural hydropower resources, could compete preferentially with three stage centrifugal compressors (with inter and aftercooling) over a range of sale prices for compressed air and a range of discount rates.

Two new promising applications of HACs were described, the first describes use a HAC as an integrated mine fan, dehumidifier and air cooler. The second adopted a HAC as part of a scheme for the separation of gas species within gaseous mixtures, and because of the generalisation of the installations away from the straightforward compression of air alone, such systems were called hydraulic gas compressors (HGCs). If used in the separation of combustion gases from fossil fuelled plant, the scheme amounts to a low-cost, low-carbon method of carbon capture that will produce high purity by-product streams of high pressure N_2.

Acknowledgements

The author expresses thanks to Dr C. Noula, Dr J. Carter, Alberto Romero and Kim Trapani for useful reviews of the manuscript. Julia Andrade helped the author understand and implement gas solubility calculations. Mr Douglas Morrison of the Centre for Excellence in Mining Innovation (CEMI), Mr Mark Passi, of Glencore's Sudbury Integrated Nickel Operations and Mr Joe Blair of Chysalix have all made observations that have also improved the presentation. Mr Chuck Arlauskis of Vale provided important inspiration and understanding of the operation of direct contact heat exchangers. The author's analysis of the work of Charles Havelock Taylor was encouraged by Mr Charlie Graham of the Canadian Mining Industry Research Organization (CAMIRO). This research was conducted as part of the Smart Underground Monitoring and Integrated Technologies (SUMIT) for Deep Mining project funded by the Ontario Research Fund, Research Excellence, Round 6 program. This support for the author and graduate students is gratefully acknowledged. Elements of this article originally appeared in a paper published in the proceedings of the 23rd World Mining Congress and are presented here with the permission of the Canadian Institute of Mining, Metallurgy and Petroleum.

References

[1] L.E. Schulze, Hydraulic Air Compressors, 1954. United States Department of Interior Information Circular 7683, May 1954.
[2] C. Dumaresq, Cobalt Mining Legacy, 2009 [online] Available at: http://www.cobaltmininglegacy.ca/power.php (accessed 15.02.13).
[3] E. Bartsch, Nickel Rim South mine: Leveraging Infrastructure for Energy Management and Optimization, 2011 [online] Presentation made at 15th ARC World Industry Forum, Orlando 2011. Available at: http://www.arcweb.com/events/arc-orlando-forum-2011/pages/ARC-Forum-Presentations.aspx (accessed 15.02.13).
[4] LeapFrog Energy Technologies Inc., Implementing a sustainable compressed air leak program – lessons learned and best practices [online] Available at: http://www.oma.on.ca/en/publications/resources/Compressed_Air_Final_070919.pdf, 2007 (accessed 21.03.12).
[5] P.L. Langborne, Hydraulic air compression: old invention – new energy source, Chart. Mech. Eng. 26 (10) (1979) 76–81.
[6] J.H. Keenan, E.P. Neumann, A simple air ejector, ASME J. Appl. Mech. 64 (1942) A75–A81.
[7] K.E. Hickman, G.B. Gibert, J.H. Carey, Analytical and Experimental Investigation of High Entrainment Jet Pumps, 1970, p. 218. NASA Report CR-1602, Washington, DC.
[8] I.W. Eames, A new prescription for the design of supersonic jet-pumps: the constant rate of momentum change method, Appl. Therm. Eng. 22 (2002) 121–131.
[9] M. Ouzzane, Z. Aidoun, Model development and numerical procedure for detailed ejector analysis and design, Appl. Therm. Eng. 23 (2003) 2337–2351.
[10] T. Narabayashi, Y. Yamazaki, H. Kobayashi, T. Shakouchi, Flow analysis for single and multi-nozzle jet pump, JSME Int. J. Ser. B 49 (4) (2006) 933–940.
[11] D.R. Stephenson, M. Cookea, A. Kowalskib, T. York, Determining jet mixing characteristics using electrical resistance tomography, Flow. Meas. Instrum. 18 (2007) 204–210.
[12] S. He, Y. Li, R.Z. Wang, Progress of mathematical modelling on ejectors, Renew. Sustain. Energy Rev. 13 (2009) 1760–1780.
[13] F. Rahman, D.B. Umesh, D. Subbarao, M. Ramasamy, Enhancement of entrainment rates in liquid–gas ejectors, Chem. Eng. Process. 49 (2010) 1128–1135.
[14] M. Worall, S. Omer, S.B. Riffat, Design analysis of a hybrid jet-pump CO_2 compression system, in: SET2010–SET209th International Conference on Sustainable Energy Technologies, 2010. Shanghai, China, 24–27 August, 2010.
[15] A. Shah, I.R. Chughtai, M.H. Inayat, Experimental study of the characteristics of steam jet pump and effect of mixing section length on direct-contact condensation, Int. J. Heat Mass Transf. 58 (2013) 62–69.
[16] C.H. Taylor, The measurement of compressed air delivered by the hydraulic compressor, Cobalt, Can. Min. Metall. Trans. 16 (1913) 210–215.
[17] C.H. Taylor, Cobalt hydraulic air compressor, Mines Minerals 30 (9) (1910) 532–534.
[18] W. Rice, Performance of hydraulic gas compressor, Trans. ASME J. Fluids Eng. 96 (1976) 645–653.
[19] G. Bidini, C.N. Grimaldi, L. Postrioti, Performance analysis of a hydraulic air compressor, Proc. Inst. Mech. Eng. A J. Power Energy 213 (1999) 191–213.
[20] G. Bidini, C.N. Grimaldi, L. Postrioti, Thermodynamic analysis of hydraulic air compressor–gas turbine power plants, Proc. Inst. Mech. Eng. A J. Power Energy 211 (A5) (1997) 429–437.
[21] W.A. Aissa, S.A.-H. Mohamed, K.A.-F. Ahmed, Performance analysis of low head hydraulic air compressor, Smart Grid Renew. Energy 1 (2010) 15–24.
[22] B.S. Field, P.S. Hrnjak, Two-phase Pressure Drop and Flow Regime of Refrigerant and Refrigerant-oil Mixtures in Small Channels, University of Illinois at Urbana-Champaign Air Conditioning and Refrigeration Centre, 2007. Report no. ACRC TR-261, p145.
[23] M.Y. Christi, M. Moo-Young, Gas holdup in pneumatic reactors, Chem. Eng. J. 38 (1988) 149–152.
[24] K. Akita, T. Yoshida, Bubble size, interfacial area and liquid-phase mass transfer coefficient in bubble columns, Ind. Eng. Chem. Process Des. Dev. 13 (1974) 84–91.
[25] P.M. Wilkinson, H. Haringa, Mass transfer and bubble size in a bubble column under pressure, Chem. Eng. Sci. 49 (1994) 1417–1427.
[26] H.J. Thorkelson, Air Compression and Transmission, McGraw-Hill, London, 1913.
[27] J.P. Frizell, Experiments on the compression of air by the direct action of water, J. Frankl. Inst. 110 (3) (1880) 145–156.
[28] P. Peele, Compressed Air Plant, fifth ed., John Wiley & Sons, New York, 1930.
[29] Anonymous, Charles Havelock Taylor (Obituary), Can. Min. Metall. Bull. (1953) 776–777.
[30] P. Bernstein, Hydraulic compressors (In German), Z. Ver. Dtsch. Ing. 54 (45) (1910) 1903–1908.
[31] R.S. Hartenberg, J. Denavit, The fabulous air compressor, Mach. Des. 32 (15) (1960) 168–170.
[32] A. Auclair, Ragged chutes, Can. Min. J. 78 (8) (1957) 98–101.
[33] B.G. Markman, The hydraulic compressor station at the Falue mine, Jernkontorets Ann. 10 (1928) 497–517.
[34] Ingersol Rand, Standard Pressure Centrifugal Air Compressors, 2013 [online] Available at: http://www.ingersollrandproducts.com/am-en/products/air/centrifugal-air-compressor/standard-pressure-centrifugal-air-compressor-/170-850-m3min-6000-30-000-cfm (accessed 26.05.13).
[35] Atlas Copco, G&P Stories, News for Customers of the Gas and Process Division, 2009. Issue 1. [online] Available at: http://www.atlascopco-gap.com/download_file.php?id=385 (accessed 26.05.13).
[36] M. Carvalho, A. Romero, G. Shields, D.L. Millar, Optimal synthesis of energy supply systems for open pit mines, Appl. Therm. Eng. 64 (1–2) (2014) 315–330.
[37] Z. Yang, Z. Wang, P. Ran, Z. Li, W. Ni, Thermodynamic analysis of a hybrid thermal-compressed air energy storage system for the integration of wind power, Appl. Therm. Eng. 66 (1–2) (2014) 519–527.
[38] S. Wang, Dynamic Simulation, Experimental Investigation and Control System Design of Gas-liquid Cylindrical Cyclone Separators, PhD Thesis, University of Tulsa, 2000.
[39] R. Sander, Compilation of Henry's Law Constants for Inorganic and Organic Species of Potential Important in Environmental Chemistry, 1999 [online] Available at: http://www.henrys-law.org/ (accessed 13.03.13).
[40] R. Battino, T.R. Rettich, T. Tominaga, The solubility of nitrogen and air in liquids, J. Phys. Chem. Ref. Data 13 (2) (1984) 563–600.

[41] L.-T. Chen, W. Rice, Properties of air leaving a hydraulic air compressor (HAC), Trans. ASME 105 (1983) 54–57.
[42] F.W. McNair, G.A. Koenig, Candle tests of air from a hydraulic air compressor, Compress. Air Mag. 16 (3) (1911) 5963–5965.
[43] USGS, National Water Information System: Web Interface, 2013. Station 04040000 Ontonagon River, Near Rockland, MI, [online], Available at: http://waterdata.usgs.gov/usa/nwis/uv?04040000 (accessed 27.09.13).
[44] E.B.W., Report on oxygen content of hydraulic air compressor at Ragged Chutes, Mines Minerals 31 (3) (1910).
[45] C. Chu, N.E. Jones, L. Allin, Linking the thermal regimes of streams in the Great Lakes Basin, Ontario, to landscape and climate variables, River Res. Appl. 26 (2010) 221–241.
[46] E. Ruckenstein, I. Shulgin, Salting-out or -in by fluctuation theory, Ind. Eng. Chem. Res. 41 (2002) 4674–4680.
[47] The Weather Network, Statistics, Station, Sudbury A, ON, Canada, 2010 [online], http://www.theweathernetwork.com/forecasts/statistics/summary/cl6068150 (accessed 01.08.10).
[48] X. Wang, Y. Hwang, R. Rademacher, Investigation of potential benefits of compressor cooling, Appl. Therm. Eng. 28 (14–15) (2008) 1791–1797.
[49] Armstrong Pumps Inc, Vortex Air Separator Models VA/VAS. Installation and Operating Instructions, 2003 [online] Available at: www.armstrongpumps.com (accessed 31.03.13).
[50] The Carbon Trust, Compressed Air, Opportunities for Businesses, 2012. Report No CVT050. [online] Available at: http://www.carbontrust.com/media/20267/ctv050_compressed_air.pdf (accessed 26.05.13).
[51] D.L. Ayers, Efficient hydraulic air compression for base loaded combustion turbines, in: Proceedings of the American Power Conference, 1991, 1991, pp. 406–412.
[52] J.L. Shapiro, The hydraulic air compression turbine, in: ASME Cogen Turbo, IGTI-Vol. 9American Society of Mechanical Engineers, New York, 1994, pp. 291–297.
[53] W.B. Giles, Hydraulic Compressor Gas Turbine Cycle, Report 80 CRD 172, General Electric Company, 1980.
[54] D. White. Hybrid Gas Turbine and Hydraulic Air Compressor System, 2003, pp. 123–131. Proceedings of ASME Turbo Expo 2003, collocated with the 2003 International Joint Power Generation Conference (GT2003) Paper no. GT2003-38131, June 16–19, 2003, Atlanta, Georgia, USA.
[55] J.A. Berghmans, F.W. Ahrens, Performance of a hydraulic air compressor for use in compressed air energy storage power systems, Trans. ASME J. Fluids Eng. Energy Syst. (1978) 213–227.
[56] S.K. Fischer, J.J. Tomlinson, P.J. Hughes, Energy and global warming impacts of not-in-kind and next generation CFC and HCFC alternatives, ORNL, 1994 [online] Available at: http://btric.ornl.gov/eere_research_reports/electrically_driven_heat_pumps/fluids_development/cfc_and_hcfc_replacements/tewi_2/tewi_2.pdf (accessed 23.03.14).
[57] J.S. Brown and P.A. Domanski, Review of alternative cooling technologies, Appl. Therm. Eng. 64 (1–2) 252–262.
[58] L.-T. Chen, W. Rice, Some psychometric aspects of a hydraulic air compressor (HAC), Trans. ASME 104 (1982) 274–276.